https://doi.org/10.5194/acp-2019-986
Preprint. Discussion started: 30 October 2019

Atmospheric Chemistry and Physics Discussions

Simulation of organic aerosol formation during the CalNex study: updated mobile emissions and simplified secondary organic aerosol parameterization for intermediate volatility organic compounds

Quanyang Lu [1,2,3], Benjamin N. Murphy [4], Momei Qin [3,a], Peter J. Adams [1], Yunliang Zhao [1,2,b], Havala O. T. Pye [4], Christos Efstathiou [5], Chris Allen [5], Allen L. Robinson [1,2]

[1] Center of Atmospheric Particle Studies, Carnegie Mellon University, Pittsburgh, PA, USA
[2] Department of Mechanical Engineering, Carnegie Mellon University, Pittsburgh, PA, USA
[3] Oak Ridge Institute for Science and Education (ORISE) Research Participant at the Office of Research and Development, U.S. Environmental Protection Agency, Research Triangle Park, NC, USA
[4] Office of Research and Development, US Environmental Protection Agency, Research Triangle Park, NC, USA
[5] General Dynamics Information Technology Research Triangle Park, North Carolina, USA
[a] Now at: Nanjing University of Information Science and Technology
[b] Now at: California Air Resources Board

Correspondence to: Allen Robinson (alr@andrew.cmu.edu) and Benjamin Murphy (murphy.benjamin@epa.gov)

Abstract. We describe simulations using an updated version of the Community Multiscale Air Quality model version 5.3 (CMAQ v5.3) to investigate the contribution of intermediate volatile organic compounds (IVOCs) to secondary organic aerosol formation (SOA) in Southern California during the CalNex study. We first derive a model-ready parameterization for SOA formation from IVOC emissions from mobile sources. To account for SOA formation from both diesel and gasoline sources, the parameterization has six lumped precursor species that account for differences in both volatility and molecular structure (aromatic versus aliphatic) of unspeciated IVOC emissions. We also implement new mobile source emission profiles that quantify all IVOCs based on direct measurements. The profiles have been released in SPECIATE 5.0. In the Los Angeles region, gasoline sources emit 4 times more non-methane organic gases (NMOG) than diesel sources, but diesel emits roughly 3 times more IVOCs on an absolute basis. When accounting for IVOCs, the model predicts all mobile sources (including on- and off-road gasoline, aircraft and on- and off-road diesel) contribute ~1 μg m^{-3} of SOA in Pasadena, CA, which corresponds to 12% of the measured SOA concentrations during CalNex. Adding mobile-source IVOCs increases the predicted SOA concentration by ~70%. Therefore, IVOCs in mobile source emissions contribute almost as much SOA as traditional precursors such as single-ring aromatics. However, addition of these emissions still does not close either the ambient SOA or IVOC mass balance. To explore the potential contribution of other IVOC sources, we perform two exploratory simulations with varying amounts of IVOC emissions from non-mobile sources. To close the mass balance of primary hydrocarbon IVOCs, IVOCs would need to account for 12% of NMOG emissions from non-mobile sources (or equivalently 30.7 Ton day^{-1} in Los Angeles-Pasadena region), a value that is well within the reported range of IVOC content from volatile chemical products. To close the SOA mass balance and explain mildly oxygenated IVOCs in Pasadena, an additional 14.8% of non-mobile source NMOG emissions would need to be IVOCs, but assigning an IVOC-to-NMOG ratio

https://doi.org/10.5194/acp-2019-986
Preprint. Discussion started: 30 October 2019


Atmospheric Chemistry and Physics Discussions

of 26.8% (or equivalently 68.5 Ton day^{-1} in Los Angeles-Pasadena region) for non-mobile sources seems unrealistically high. By incorporating the most comprehensive mobile emissions profiles for SVOCs and IVOCs along with experimentally constrained SOA yields from mobile IVOCs, this CMAQ configuration represents the most accurate photochemical model prediction of the contribution of mobile sources to urban and regional ambient OA to date. Our results highlight the important contribution of IVOCs to SOA production in Los Angeles region, but also underscore that other uncertainties must be addressed (multigenerational aging, aqueous chemistry, and vapor wall losses) to close the SOA mass balance. This research also highlights the effectiveness of regulations to reduce mobile source emissions, which have, in turn, increased the relative importance of other sources, such as volatile chemical products.

https://doi.org/10.5194/acp-2019-986
Preprint. Discussion started: 30 October 2019


Atmospheric Chemistry and Physics Discussions

1 Introduction

Exposure to fine particulate matter ($PM_{2.5}$ and PM_1) has been associated with increased mortality, lung cancer and cardiovascular diseases (Apte et al., 2018; Di et al., 2017). Organic aerosol (OA) is a major component of ambient fine particulate matter (Jimenez et al., 2009; Zhang et al., 2015). The majority of OA, even in most urban areas, is secondary organic aerosol (SOA), formed from the atmospheric oxidation of gas-phase species. Over the past several decades, primary emissions have been greatly reduced in the United States, which has led to significant improvement in air quality, especially in the Los Angeles basin in California (Warneke et al., 2012; Zhang et al., 2018). However, SOA remains an important component of fine particulate matter, but its sources are uncertain (Ensberg et al., 2014; McDonald et al., 2018).

Intermediate volatility organic compounds (IVOCs) are an important class of SOA precursors (Chan et al., 2009; Liggio et al., 2016; Presto et al., 2009; Zhao et al., 2014). IVOCs, for example, C_{12} to C_{17} *n*-alkanes and polycyclic aromatic hydrocarbons, are efficient SOA precursors (Chan et al., 2009; Presto et al., 2010a). In addition, chamber experiments using unburnt fuel and diluted exhaust have demonstrated the importance of IVOCs to SOA production from mobile source emissions (Gordon et al., 2014; Jathar et al., 2013; Miracolo et al., 2011; Platt et al., 2017).

Despite this evidence, IVOCs are not routinely or consistently accounted for in chemical transport models. A major challenge has been the lack of emissions data due to a combination of sampling challenges and the fact that the vast majority of IVOC emissions have not been speciated on a molecular basis. In addition, chemical mechanisms (e.g. SAPRC, Carbon Bond, etc.) often do not explicitly account for IVOCs, instead lumping them with VOCs or non-reactive gases. Several recent studies report total (speciated and unspeciated) IVOC emissions from a variety of mobile sources, including on- and off-road gasoline, diesel, aircraft and vessel engines (Cross et al., 2013; Huang et al., 2018; Kroll et al., 2014; Pereira et al., 2018; Presto et al., 2011; Wang et al., 2012; Zhao et al., 2015, 2016). In addition to measuring total emissions, recent studies also provide insight into the molecular structure of the IVOCs (Drozd et al., 2019; Hatch et al., 2017; Hunter et al., 2017; Worton et al., 2014). For example, IVOCs in diesel exhaust are primarily comprised of aliphatic compounds while IVOCs in gasoline exhaust are primarily aromatics with higher OH reaction rates and SOA yields. Zhao et al. (2015, 2016, 2017) used these new emissions data to explain the SOA formation in smog chamber experiments with diluted vehicle emissions. However, the SOA mechanism proposed by Zhao et al. (2015, 2017) includes 79 different classes of IVOCs, which is too computationally expensive for implementation in current operational CTM.

Because of the high levels of both ozone and PM exposure in the Los Angeles basin over the last several decades, extensive ambient measurement campaigns have explored the sources of poor air quality in the region, including the CalNex campaign in 2010 (Ryerson et al., 2013). During the CalNex campaign, average OA at the Pasadena supersite was 7 $\mu g\ m^{-3}$, of which SOA, defined as the sum of semi-volatile and low-volatile oxygenated OA (SV-OOA and LV-OOA) factors from AMS analysis, contributed 66% to total OA mass (Hayes et al., 2013). Zhao et al. (2014) measured the ambient IVOC concentration at the Pasadena site, and estimated that photo-oxidation of IVOCs contributed up to 57% of SV-OOA during CalNex.

https://doi.org/10.5194/acp-2019-986
Preprint. Discussion started: 30 October 2019


Atmospheric Chemistry and Physics Discussions

A number of chemical transport model (CTM) studies have examined SOA formation in the LA basin during the CalNex campaign (Baker et al., 2015; Fast et al., 2014; Jathar et al., 2017; Murphy et al., 2017; Woody et al., 2016). However, these studies used very different assumption for IVOC emissions and their SOA yields. IVOC emissions are commonly estimated by applying a scaling factor to some other species (most commonly POA). These scaling factors have been based on little experimental data and the typically the same factor is applied to all sources. For example, Fast et al. (2014) assumed additional SOA precursor (IVOC and/or SVOC; semivolatile organic compounds) mass of 6.5 × POA and Woody et al. (2016) assumed 7.5 × POA based on previous estimations (Hodzic et al., 2010; Koo et al., 2014), applied to all emission source categories. Jathar et al. (2017) assumed mobile IVOC emission as 25% of diesel NMOG emissions and 20% of gasoline NMOG emissions. Finally, Baker et al. (2015) did not explicitly account for IVOCs, but increased the SOA yields from VOCs by a factor of four compared to the base CMAQ version. Despite these efforts, these studies still underpredicted the measured OA by a factor of 2 to 6 (Hayes et al., 2013). Murphy et al. (2017) largely closed the OA mass balance by defining a new lumped SOA precursor called potential combustion volatile organic compounds (pcVOC) with emissions equal to 9.6 × POA and an SOA yield of 1. However, all the above-mentioned models used scaling factors that are not based on actual emission data. They also only use a single IVOC surrogate, which does not account for differences in IVOC chemical composition. Lu et al. (2018) showed that a single scaling factor does not represent the magnitude of actual IVOC emissions across all mobile sources. Finally, none of these models account for the effects of differences in molecular structure in IVOC emissions on SOA yield.

Mobile sources are major sources of NMOG emissions, and therefore important sources of SOA precursors in urban environments (Gentner et al., 2017). Historically, mobile sources have been the dominant source of NMOG in many urban areas, but their contribution has been reduced due to increasingly stringent emission regulations. They currently contribute 32% of the anthropogenic VOC emissions nationally (and 43% in Los Angeles county) as reported in the 2014 EPA National Emission Inventory (NEI). In Los Angeles county, on- and off-road gasoline and diesel sources account for more than 96% of mobile-source emission.

Lu et al. (2018) recently compiled mobile-source emission data, including on- and off-road gasoline, aircraft and diesel engines, to create updated model-ready emission profiles that include IVOCs. They found that mobile source NMOG emissions can be explained by trimodal distributions of by-product, fuel and oil modes. IVOC emissions originate from fuel components with 'enrichment' effects found in all gasoline, aircraft and diesel-source exhausts (Cross et al., 2013, 2015; Presto et al., 2011; Zhao et al., 2018). This applies to both low emitting heavily controlled sources (e.g. LEV-II certified gasoline vehicle) and uncontrolled high sources (e.g. two stroke gasoline off-road sources) (Lu et al., 2018). Therefore, in this work, mobile IVOC emissions are modelled and grouped based on fuel type usage.

In this paper, we use an updated version of CMAQv5.3 to investigate the sources and contribution of SVOCs and IVOCs to SOA formation in the Los Angeles region during the CalNex campaign. We updated CMAQv5.3 with a new set of mobile-source NMOG and SVOC emission profiles that include 6 classes of IVOCs and a new parameterization of SOA formation from IVOC precursors that is suitable for implementation into a chemical transport model. The new emission

https://doi.org/10.5194/acp-2019-986
Preprint. Discussion started: 30 October 2019


Atmospheric Chemistry and Physics Discussions

profiles are based on the direct measurement of IVOCs from on- and off-road mobile sources (Gordon et al., 2013; Lu et al., 2018; May et al., 2014; Presto et al., 2011; Zhao et al., 2015, 2016). These profiles (100VBS to 103VBS) are now available in SPECATE 5.0 (US EPA, 2019). The new SOA parameterization is derived from a comprehensive parameterization that explains the SOA formation from dilute mobile source exhaust in smog chamber studies (Zhao et al., 2015, 2017). We evaluate the resulting model, now the most up-to-date representation of mobile source organic compound emissions using data collected during the CalNex campaign, including direct measurements of ambient IVOCs. Finally, we explore potential contribution of non-mobile sources to IVOC and OA concentrations.

2 Parameterizing SOA formation from mobile-source IVOCs

Mobile sources are comprised of a complex mixture of on- and off-road sources, including gasoline, aircraft and diesel engines. However, they are predominantly gasoline- and diesel-powered, with a small fraction of aircraft emissions. In the NEI 2014, gasoline sources contribute 90% mobile sources of national NMOG emissions, diesel sources contribute 8% followed by 1% from aircraft. In this work we apply the source profiles of Lu et al. (2018) to estimate the IVOC emissions for different mobile sources. Note that the IVOCs are normalized to NMOG emissions, which only includes the organics in volatility range from $C^* = 10^3$ to 10^{11} μg m^{-3}. Table 1 summarizes the IVOC-to-NMOG ratios for different mobile sources. The ratios (and associated emission profiles) vary widely depending on the underlying fuel. For gasoline, aircraft to diesel sources, NMOG emissions are 4.6%, 28.5% and 55.5% IVOCs, respectively. Weighting NMOG emissions by the IVOC fractions, mobile-source IVOC emissions in the Los Angeles basin are 44% from gasoline, 51% diesel and 5% aircraft. IVOC emissions from gasoline source include high fractions of aromatics (Drozd et al., 2019; Zhao et al., 2016).

We developed a simplified parameterization to simulate SOA formation from IVOCs. It is derived from the model of Zhao et al. (2015, 2016), which explicitly accounts for 79 different classes of IVOCs. The chemistry and transport associated with 79 additional species in the gas and particle phase would be too computationally expensive in a CTM which normally has about 50 or less organic aerosol species. The Zhao et al. (2015, 2016) model accounts for 57 individual IVOCs and 22 lumped IVOCs. The 22 lumped IVOCs are comprised of unspeciated IVOCs grouped based on gas chromatography (GC) retention time and an assigned chemical class based on its mass spectra. This model explains the SOA formation from dilute exhaust of gasoline and diesel vehicles measured in chamber experiments (Zhao et al., 2015, 2017). Our simplified SOA parameterization accounts for the key differences in chemical composition of the IVOC emissions from different mobile sources. This is important because the composition of the IVOC emissions varies by source class (e.g. gasoline versus diesel) and SOA yield depends on both molecular weight (volatility) and chemical structure (aromatics versus alkanes) (Chan et al., 2009; Jathar et al., 2013; Lim and Ziemann, 2005, 2009; Presto et al., 2010a). For example, diesels emit more lower volatility IVOCs than gasoline engines, but diesel IVOC emissions are mainly comprised of aliphatic compounds versus aromatics for gasoline. These differences matter because, for a given chemical class, SOA yields generally increase with increasing molecular weight, which increases the effective SOA yield of diesel exhaust relative to

https://doi.org/10.5194/acp-2019-986
Preprint. Discussion started: 30 October 2019

Atmospheric Chemistry and Physics Discussions

gasoline exhaust. However, for a given carbon number, the SOA yield for hydrocarbon IVOCs generally follows aromatics > cyclic > linear > branched alkanes (Lim and Ziemann, 2009; Tkacik et al., 2012), thus gasoline IVOC yields increase when their structure is considered. Finally, aromatic IVOCs have higher OH reaction rates than alkanes (Chan et al., 2009; Zhao et al., 2017).

To illustrate the challenge, Figure 1 plots the SOA yield (expressed as SOA mass divided by mass of precursor) as a function of volatility for the 79 different IVOCs in the model of Zhao et al. (2015, 2016) at a typical atmospheric OA concentration of 10 μg m^{-3}. This model likely provides a conservative estimate for SOA yields of lower volatility IVOCs, as $C_{18\text{-}22}$ *n*-alkanes are assumed to have the same SOA yields as C_{17} *n*-alkanes. The scatter in the data highlights the complex relationship between molecular structure and SOA yield.

Our goal is to derive a semi-empirical SOA parameterization with the minimum number of surrogate species that reproduces the mechanism of Zhao et al. (2015, 2016). The simplified parameterization must account for the differences in SOA formation from IVOC emissions from different mobile source categories (gasoline, diesel and aircraft). We developed the simplified parameterization using the volatility basis set (VBS) framework of Donahue et al. (2006) following the approach of Presto et al. (2010b). Briefly, to simulate SOA formation, each lumped IVOC group reacts with OH to form a set of semi-volatile products in Eq. (1):

$$IVOC_i + OH \rightarrow \alpha_{i,1}P_{C^*=0.1} + \alpha_{i,2}P_{C^*=1} + \alpha_{i,3}P_{C^*=10} + \alpha_{i,4}P_{C^*=100} \quad \text{for group } i = 1 \text{ to } 6 \qquad (1)$$

where $\alpha_{i,1}$ to $\alpha_{i,4}$ are mass-based stoichiometric coefficients distributing the reaction products across a second volatility basis set from 0.1 to 100 ug/m^3 (Presto 2010b). For each lumped IVOC species there are 5 unknowns: four stoichiometric coefficients ($\alpha_{i,1}$ to $\alpha_{i,4}$) and the OH reaction rate $k_{OH,\,i}$. These coefficients and reaction rates are derived by fitting the mechanism of Zhao et al. (2015, 2016). All SOA parameters are set at fixed temperature of 298 K. Details of the fitting procedure are in the SI.

We initially tried using four lumped-IVOC-species distributed across the volatility basis set (C* = 10^3 to 10^6 ug/m^3) to account for the influence of precursor volatility (molecular size) on SOA yield. However, that model poorly reproduced the SOA formation from gasoline vehicle emissions, especially at shorter time scales (Figure S1). The problem is that IVOCs in diesel exhaust are dominated by aliphatic compounds while IVOCs in gasoline exhaust are dominated by aromatics (Drozd et al., 2019; Zhao et al., 2016); as previously discussed, aromatics compounds have different OH reaction rates and SOA yields (Figure 1) (Lim and Ziemann, 2009; Tkacik et al., 2012).

We therefore defined two additional lumped IVOC species with C* = 10^5 and 10^6 μg m^{-3} to account for the aromatic IVOCs in engine exhaust (Table 1). Mobile-source IVOC emissions in the lower volatility bins of C* = 10^3 and 10^4 μg m^{-3} are primarily alkanes from unburnt fuel or lubricant oil (Lu et al., 2018; Worton et al., 2014); we therefore only include one lumped aliphatic IVOC species in each of those bins.

To illustrate the performance of the new parameterization, Figure 2 (a) compares the predicted SOA using our six-IVOC-group parameterization to the original mechanism of Zhao et al. (2015, 2016). It shows that the two models agree with an absolute error less than 0.01 for all mobile sources at OA = 5 μg m^{-3}. Across a wide range of atmospherically relevant

https://doi.org/10.5194/acp-2019-986
Preprint. Discussion started: 30 October 2019


Atmospheric Chemistry and Physics Discussions

concentrations (OA = 1 to 50 μg m^{-3}), Figure 2(b) shows that the relative error is less than 6% between our new parameterization and the original mechanisms of Zhao et al. (2015, 2016). The new parameterization captures the fact that gasoline IVOC emissions are mostly aromatics (Drozd et al., 2019; Zhao et al., 2016) and therefore have higher SOA production in the first 10 hours compared to aircraft and diesel IVOC emissions. It also predicts that diesel IVOC emissions have the overall highest SOA yield due to their lower volatility compounds (Lu et al., 2018; Zhao et al., 2015).

Table 2 lists the set of k_{OH} and α_i for the simplified six-IVOC-group parameterization for mobile source emissions. Molecular weights (MW) are determined as the average MW of *n*-alkanes or speciated aromatics in each volatility bin. Enthalpy of vaporization (H_{vap}) are determined using the fitted parameterization in Ranjan et al. (2012). In this work, we implement this six-lumped-IVOC-group parameterization to model IVOC SOA formation in CMAQ v5.3.

3 CMAQ model configuration

To evaluate contribution of mobile source IVOC emissions to ambient SOA, we implement our new six-IVOC-group SOA parameterization and emissions profiles into CMAQ v5.3. We used the model to simulate the air quality in California from 1 May to 30 June 2010, which includes the entire CalNex campaign (May and July 2010). Except as noted below, the simulations described here have essentially the same modelling domain and input parameters as the previous modelling studies on CalNex (Baker et al., 2015; Murphy et al., 2017; Woody et al., 2016).

3.1 Model configuration

The model domain covered California and Nevada with a 4 km (325×225) grid resolution, with 35 vertical layers. The input meteorology and NEI emission inventory are similar to those used by Baker et al. (2015), Woody et al. (2016) and Murphy et al. (2017) and are remade in this work and Qin et al. (2019). Meteorological inputs were generated using the Weather Research and Forecasting Model (WRF) Advanced Research WRF core version 3.8.1 (Skamarock et al., 2008) with one additional model layer at the surface compared to previous studies (i.e. the lowest layer of approximately 40 m depth has been split into two 20 m deep layers to better resolve surface gradients). The emissions inputs are based on the 2011 NEI version 2 with mobile, wildfire, and electric generating point source emissions calculated for 2010. Mobile on-road and non-road emissions are calculated by MOVES 2014a. Biogenic emissions are calculated online with BEISv3.61 and improved land use cover from BELD4 (Bash et al., 2016). Sea-spray aerosols are calculated online and incorporate dynamic prediction of particle population size and standard deviation. Wind-blown dust emissions are neglected and should not impact comparisons with the data collected by the AMS, which detects non-refractory particulate compounds. Gas-phase chemistry is simulated with the SAPRC07T chemical mechanism (Carter, 2010; Hutzell et al., 2012; Xie et al., 2013). Aerosols are simulated using the Aero-7 module (CMAQ-AE7) with monoterpene photo-oxidation updates (Xu et al., 2018) and organic water uptake (Pye et al., 2017). Boundary conditions were generated from a 12 km continental U.S. simulation of April-June 2010. We use the first 14 days of the simulation as a spin-up to minimize the influence of initial conditions.

https://doi.org/10.5194/acp-2019-986
Preprint. Discussion started: 30 October 2019


Atmospheric Chemistry and Physics Discussions

3.2 POA emissions

Semi-volatile POA includes both SVOC and lower volatility organics in the comprehensive organic emission profiles (Lu et al., 2018). In CMAQ v5.3, the volatility profile of Robinson et al. (2007) is used to represent all combustion sources. Here, we update the volatility distribution for mobile POA using the new mobile emission profiles in Lu et al. (2018). The profiles (8873VBS, 8992VBS to 8996VBS) are also available in SPECIATE 5.0 (US EPA, 2019). For non-mobile combustion sources, we use the biomass burning POA volatility distribution from May et al. (2013b) for wood-burning sources, cooking OA volatility distribution as in Woody et al. (2016) for cooking sources, and diesel POA volatility distribution from May et al. (2013a) as a surrogate for other combustion sources. Table 3 summarizes the volatility distributions and scaling factors used in this work. The POA emissions were the same in all model runs.

A challenge is that most existing POA emission factors used to inform inventories such as NEI are based on filter measurements, which do not quantitatively collect all SVOCs. For example, filters collect only a portion of SVOC vapors. Estimating this error is complex because there are competing biases. First, source testing is often performed at low levels of dilution which creates high concentrations (relative to the more dilute atmosphere) that shifts gas-particle partitioning of SVOCs to the particle phase. In these situations, filters collect a larger fraction of SVOCs than more dilute conditions (of course, at high enough concentrations, filters will also collect some IVOC vapors). Second, during mobile source testing, filters are commonly collected at elevated temperatures (e.g. 47 ºC) to avoid water condensation, which shifts gas-particle partitioning towards the gas phase, reducing the fraction of SVOCs collected by a filter. Finally, filters collect some vapors as sampling artifacts, which depends on many factors, including filter material, filter face velocity, and filter pre-treatment (Subramanian et al., 2004). Therefore, the fraction of SVOCs collected by filters depends on these competing effects, which are difficult to quantify. As expected, data from Zhao et al. (2015, 2016) and Lu et al. (2018) indicate that the fraction of SVOC collected depends on the OA concentration inside the sampling system.

To estimate the potential SVOC vapors in the filter-based POA emission factor measurements, we compared the mass of lower volatility organics (SVOC + LVOC + NV) collected on filters and Tenax tubes versus the mass collected on filters (regular POA measurement) (Lu et al., 2018). Although results for all fuel types indicated an SVOC filter artifact correction factor greater than 1 should be applied, the diesel and gas-turbine tests were within 10% of unity, which is within experimental uncertainty. Therefore, we did not add any SVOC mass to these emissions. For gasoline sources with generally lower emissions (and therefore gas-particle partitioning shifted more to the vapor phase), the data indicate an average bias of 40%, which means that lower volatility organics were only partially collected by the filter. We therefore applied a filter artifact correction factor of 1.4 to gasoline POA emissions, as shown in Table 3.

The POA model, similar to the 1.5-VBS of Koo et al. (2014) contains five pairs of SVOC vapor/particle species, with O:C increasing slightly with decreasing volatility. POA emissions are then distributed into these species and are susceptible to multigenerational aging, as described in Murphy et al. (2017). Briefly, the approach predicts the reaction of SVOCs with hydroxyl radical and distributes the product mass to a second set of five vapor-particle pairs at moderate O:C

https://doi.org/10.5194/acp-2019-986
Preprint. Discussion started: 30 October 2019


Atmospheric Chemistry and Physics Discussions

values. The stoichiometric ratios applied to the product mass were derived to match the SOA enhancement predicted by a full 2D-VBS simulation of the simultaneous functionalization and fragmentation of SVOCs. No changes were made to the chemical properties (e.g. carbon number, O:C, etc.) or reaction stoichiometry from Murphy et al. (2017).

3.3 IVOC emissions

The main difference from previous implementations of CMAQ to simulate the CalNex campaign (Baker et al., 2015; Murphy et al., 2017; Woody et al., 2016) is the new mobile IVOC emission data and the application of the six-IVOC-species SOA parameterization. Mobile sources contribute more than 40% of anthropogenic NMOG emissions in the South Coast Air Basin in the CalNex emission inventory (Baker et al., 2015). Given the consistency of the speciation and IVOC-to-NMOG ratio for sources using same type of fuel (Lu et al., 2018), we assign base mobile emission source profiles based on fuel type (gasoline, diesel, or jet fuel). NMOG emissions from all on- and off-road gasoline sources are represented using the same average gasoline exhaust profile. NMOG emissions from all on-road, off-road diesel sources and rail are represented using the same average diesel exhaust profile. NMOG emissions for all jet-fuelled sources are represented using the same gas-turbine exhaust profile (Lu et al., 2018). The IVOC components of these profiles are summarized in Table 1 and complete profiles are given in SPECIATE 5.0 (US EPA, 2019). Total IVOC emissions are determined using the IVOC-to-NMOG ratios, which are more consistent across source types than IVOC-to-POA ratios (Lu et al., 2018).

For this work IVOC emissions are added to existing NMOG emissions. This was done to keep the VOC emissions constant in order to isolate the contribution of IVOCs to SOA. However, Lu et al. (2018) argues that existing NMOG inventories largely include IVOCs, just that they are misattributed to VOCs. Therefore, we should have proportionally reduced the VOC emissions to keep the overall NMOG emissions (VOC + IVOC) constant. Not changing the VOCs emissions minimally effects the OA model evaluation, because total traditional anthropogenic VOCs only contribute 0.2 μg m^{-3} SOA at Pasadena during the CalNex campaign (Baker et al., 2015). The SVOC products of IVOC oxidation that can then form SOA are also susceptible to aging and are treated here with the same mechanism as the oxygenated SVOCs from POA aging. In this way, fragmentation and functionalization are accounted for, albeit with uncertainty. Because IVOC products are expected to have lower carbon numbers than products of primary SVOC oxidation, our approach here may represent an upper bound on the potential for IVOC SOA aging to further enhance particle mass.

3.4 Simulation cases

To systematically explore the effect of adding IVOC emissions from mobile and non-mobile sectors, we performed four simulation cases, summarized in Table 4. All cases use the same emission inputs described earlier, and POA emissions are modelled with the new volatility distributions and filter artifact correction factors as described in Section 3.3. Table 4 shows the difference in total anthropogenic POA emission before and after assigning the filter artifact correction factor of 1.4 on gasoline POA emissions. The base case (Case 1) assumes mobile SOA are only formed through the oxidation of traditional VOC emissions and SVOCs from combustion POA evaporation.

https://doi.org/10.5194/acp-2019-986
Preprint. Discussion started: 30 October 2019


Atmospheric Chemistry and Physics Discussions

Figure 3(a) compares the anthropogenic NMOG emissions in the Los Angeles Basin region (geographical boundaries are defined by simulation grid cells shown in Figure S2). In the base case (Case 1), mobile sources contribute 43% of anthropogenic NMOG emissions, of which gasoline sources contribute 35%, diesel sources contribute 8% and aircraft less than 1%. Non-mobile sources contribute the rest of 57% anthropogenic NMOG emissions, of which VCP usage contributes 39%, followed by 17% from other sources. There are negligible cooking and biomass burning NMOG emissions during CalNex (1.5%).

We then incrementally add mobile IVOC emissions to the model. Table 4 shows that Case 2 adds on average 27.6 Ton/day mobile source IVOC emissions. The difference between (2) and (1) is the SOA contribution from mobile emitted IVOCs. In Case 3 and 4, we then incrementally add IVOC emissions from non-mobile to explore the contribution of non-mobile sources of IVOCs as discussed in Section 4.2.

4 CMAQ simulation results

To evaluate the updated model performance, we compared model predictions to measured data from the CalNex campaign at Pasadena, CA, as well as the organic carbon (OC) measured at the Chemical Speciation Network (CSN) sites in California. The CalNex campaign characterized atmospheric composition at two sites in southern California, Pasadena, and Bakersfield, from 15 May to 29 June 2010 (Ryerson et al., 2013). We focus on the Pasadena site, which is located 18 km northeast and generally downwind of downtown Los Angeles, in particular because there were direct measurements of IVOCs (Zhao et al., 2014). We also evaluate model predictions at the Pasadena site for OA, BC, CO, speciated VOCs and Planetary Boundary Layer (PBL) height.

4.1 Base case and mobile IVOC case

4.1.1 IVOC mass concentrations

Figure 3(b) compares the model-predicted and measured campaign-average IVOC mass concentration at the Pasadena site. Zhao et al. (2014) reported data for two classes of IVOCs differentiated based on mass spectral signature: hydrocarbon IVOCs and mildly oxygenated IVOCs. Zhao et al. (2014) attributes hydrocarbon IVOCs to primary emissions; the mildly oxygenated IVOC could either be primary emissions or formed via atmospheric oxidation. The CalNex campaign-averaged measured hydrocarbon IVOCs at the Pasadena site was 6.3 μg m^{-3}; the measured mildly oxygenated IVOC concentration was 4.2 μg m^{-3}.

The base case predicts essentially no IVOC concentration as they are not explicitly included in the model (though could be implicitly included in the mass of some VOC species). Case 2 (mobile IVOC case) only predicts 2.4 μg m^{-3} of IVOCs at the Pasadena site, which corresponds to 38% of measured hydrocarbon IVOCs. This indicates that mobile emissions are an important source of IVOCs in the LA region, but more than half of the hydrocarbon IVOCs measured in

https://doi.org/10.5194/acp-2019-986
Preprint. Discussion started: 30 October 2019

Atmospheric Chemistry and Physics Discussions

Pasadena are likely from non-mobile sources. In addition to hydrocarbon IVOCs, Zhao et al. (2014) measured 4.2 ug m^{-3} of mildly oxygenated IVOCs, which are also not explained by mobile-source emissions.

While the comparison in Figure 3b suggests that there are other (non-mobile) important sources of IVOC, there are a number of uncertainties present in this estimate, including (1) uncertainty in mobile source activity, (2) uncertainty in mobile source NMOG emission factors, and (3) uncertainty in IVOC-to-NMOG emission ratios.

The first potential uncertainty is mobile-source activities: BC and CO are commonly used as indicators of gasoline and diesel sources activity. The mobile-source CO emission inventory in LA basin during CalNex is correctly modelled (Kim et al., 2016). The model performs well for CO, but BC concentrations are overestimated by a factor of 2 (Figure S3). These comparisons suggest that gasoline activity (the major of source of CO) is modelled correctly, with over-estimation in diesel activity or the diesel BC emission factor (the major source of BC). The second type of potential uncertainty is from mobile-source NMOG emission factors. May et al. (2014) suggest that EMFAC emission factors (which are used to create the mobile source emission inventory for these simulations) are robust, except for LEV-2 vehicles. During the 2010 CalNex period, MOVES 2014 (USEPA, 2014) estimates LEV-2 vehicles (considering model year after 2004) only emit 9% of total gasoline NMOG emissions in California and therefore are not major contributors in mobile emissions. The final potential explanation for uncertainty is the IVOC-to-NMOG ratios. Zhao et al. (2016) and Lu et al. (2018) show that IVOC-to-NMOG ratios of cold-start UC (unified cycle) emissions from gasoline sources are consistent across a large number of vehicles spanning a range of emission certification standards. Although gasoline vehicle hot-running IVOC emissions are enriched by as much as a factor of 4 compared to the cold-start UC cycle (Lu et al., 2018; Zhao et al., 2016), EMFAC2017 estimates that running exhaust only contributes 34% of total gasoline summertime NMOG emissions in CA state-wide in 2010. A simple weighted average of 66% emission using cold-start UC emission profile and 34% of emission using hot-running emission profile increases the IVOC-to-NMOG fraction by a factor of 2, from 4.5% to 9.1%. The IVOC-to-NMOG ratio for diesel sources is already high (55%) and thus it cannot be increased as much as the gasoline emissions (less than a factor of 2). Therefore, the largest uncertainty in modelled mobile IVOCs is the modelled gasoline source IVOC-to-NMOG ratio, which could be underestimated by as much as a factor of two. This means that the overall uncertainty in modelled mobile IVOC emissions is less than a factor of 2. This would improve the hydrocarbon IVOCs prediction, but it seems likely that uncertainties are not large enough to close the ambient IVOC mass balance.

Jathar et al. (2017) also updated CMAQ with mobile-source IVOC emissions estimates. They assumed that IVOCs contribute 25% and 20% of the NMOG emissions from gasoline and diesel source, respectively. However, these ratios are not based on direct measurements, but instead inferred from SOA closure studies for chamber experiments. The model of Jathar et al. (2017) predicted mobile sources contribute 3.9 μg m^{-3} of IVOCs, which is about factor of 1.5 higher than the IVOC concentrations predicted here and explained 65% of measured ambient hydrocarbon IVOC concentrations. The better closure is due the very high IVOC-to-NMOG ratio assumed for gasoline vehicles, which is not supported by direct measurements (Drozd et al., 2019; Zhao et al., 2016).

https://doi.org/10.5194/acp-2019-986
Preprint. Discussion started: 30 October 2019

Atmospheric Chemistry and Physics Discussions

335 **4.1.2 Primary VOC/IVOC diurnal patterns**

Figure 4 compares the measured and modelled campaign-average diurnal patterns of important anthropogenic VOCs (benzene, toluene, m-/p-/o- xylenes) and hydrocarbon IVOCs. Measured concentrations of benzene, toluene and hydrocarbon IVOCs are highest in the early afternoon (12pm - 2pm, in Figure 4 a, b and d). This has been attributed to the transport of morning emissions from downtown Los Angeles to Pasadena (Borbon et al., 2013). Measured xylene
340 concentrations show a slight decrease in daytime, which is attributed to their relatively high OH reaction rate and thus faster oxidation during the daytime (de Gouw et al., 2018).

Figure 4 indicates that the model is able to reproduce the measured benzene diurnal pattern while failing to reproduce the toluene, xylene and hydrocarbon IVOC diurnal patterns. Figure 4 (b and c) shows that during night-time the model overpredicts toluene and xylene concentrations by a factor of 2 and 1.4, respectively. Modelled hydrocarbon IVOCs
345 mass concentration (Case 2) are underestimated throughout the day (Figure 4d and Figure 3b).

Figure 4 also indicates that concentrations of all modelled species peak at around 6 AM and steadily decrease from 6 AM to 4 PM, in contrast to the early-afternoon peaks (12 PM to 2 PM) in measured data. A potential explanation is that the model is incorrectly simulating the PBL height. On average, the measured PBL height ranges from ~200 m at night to ~900 m at noon, while modelled PBL height ranges from ~60 m at night and up to 1500 m at noon (Figure S4). Therefore, the
350 model likely overestimates the PBL dilution in Pasadena, which impacts concentrations of all species, and contributes to the poor diurnal pattern model performance shown in Figure 4.

4.1.3 OA mass concentration and SOA/POA diurnal patterns

Figure 5(a) plots the AMS-measured (black line) and CMAQ-modelled (color lines) hourly-averaged PM_1-OA time series in Pasadena site during CalNex. We consider the Pearson's correlation coefficient (r) and root-mean-square error (RMSE) as
355 the evaluation metrics between measured and model OA time series. The definitions of r and RMSE are shown in Eq. (2) and (3):

$$r = \frac{\mathrm{Cov}\,(OA_{measured}, OA_{model})}{\mathrm{Var}(OA_{measured})\,\mathrm{Var}(OA_{model})} \quad (2)$$

$$\mathrm{RMSE} = \sqrt{\frac{\sum_{i=1}^{N}(OA_{measured} - OA_{model})^2}{N}} \quad (3)$$

Our base model (Case 1) significantly underpredicts the OA concentration, often by more than a factor of 3, over the entire
360 time period. Case 1 prediction has a large RMSE = 5.3 μg m^{-3}, which is comparable to the average measured OA (6.9 μg m^{-3}), and moderate positive correlation (r = 0.69).

Figures 5(b) and (c) compare the modelled average diurnal patterns for SOA and POA (lines) to AMS-measured (boxplots) OOA (SV-OOA + LV-OOA) and (HOA + COA) factors (Hayes et al., 2013). The measured OOA factor in Figure 6(b) has a strong peak in the early afternoon, similar to the OH radical concentration (de Gouw et al., 2018) and photo-
365 chemical age (Hayes et al., 2015).

https://doi.org/10.5194/acp-2019-986
Preprint. Discussion started: 30 October 2019


Atmospheric Chemistry and Physics Discussions

Figure 5(b) shows that Case 1 produces very little SOA from VOCs, similar to previous simulations with the base version of CMAQ (Baker et al., 2015; Woody et al., 2016). In Case 1, the modelled peak SOA concentration is 1.65 μg m^{-3} at the Pasadena site, which is 5 times lower than the AMS-measured value (8.63 μg m^{-3}). Both modelled LV-OOA and SV-OOA are much lower than AMS-measured factors.

Figure 2 indicates that IVOC emissions contribute greatly to SOA formation, especially the day-time SOA peak concentration due to their high SOA yield and OH reaction rates. In Case 2, the addition of mobile IVOC emissions increases peak SOA concentration by 60%, from 1.65 to 2.75 μg m^{-3} and daytime SOA enhancement ($SOA_{peak} - SOA_{night}$) by 110% from 0.82 to 1.73 μg m^{-3}. The increase in SOA at night from IVOC oxidation was about a factor of 4 smaller than the daytime enhancement, therefore, IVOC emissions contribute more daytime SOA enhancement than night-time SOA (background). Adding mobile-source IVOC improves model performance, but Case 2 still only explained 32% of AMS-measured daytime peak SOA.

Figure 5(c) shows that the model predicts POA average concentrations (modelled: 1.73 μg m^{-3} vs measured: 2.01 μg m^{-3}) and diurnal patterns well, with the filter artifact corrected POA emissions (1.4 × POA) from gasoline sources and updated POA volatility distributions for other mobile and non-mobile sources (Table 3). This indicates that the POA volatility distributions and primary emissions are representative.

To summarize, Case 2 (mobile IVOC) moderately improves the model predictions of hydrocarbon IVOC and SOA concentrations, but does not close the mass balance for hydrocarbon IVOCs or SOA. In the next section, we explore the potential contribution of IVOC emissions from non-mobile sources (McDonald et al., 2018).

4.2 Non-mobile IVOC cases

4.2.1 IVOC mass concentrations and diurnal pattern

Motivated by recent work on volatile chemical products (VCPs) (Khare and Gentner, 2018; McDonald et al., 2018), we also investigated potential IVOC emission from non-mobile source. For example, McDonald et al. (2018) estimated that 19.6% of total gas-phase VCP emissions are IVOCs. Khare and Gentner (2018) reported IVOC content range from 0 to 95% in 12 commercially available VCPs. However, many of these IVOCs are heavily oxygenated.

Figure 3(b) shows that the total campaign-average measured IVOC concentrations were 10.5 μg m^{-3} (6.3 μg m^{-3} of hydrocarbon IVOCs and 4.2 μg m^{-3} mildly oxygenated IVOCs) (Zhao et al., 2014). This is a lower bound estimate of ambient oxygenated IVOCs, because oxygenated species only partially eluted from the GC column used for the analysis (Zhao et al., 2014). The source of these oxygenated IVOCs is unknown; they could be from primary emissions (e.g. VCPs) and/or secondary production of VOC/IVOC oxidation.

Cases 3 and 4 explore different levels of IVOC emission for non-mobile sources. The IVOC-to-NMOG ratios are not based on independent laboratory data, but are set to close the gap between modelled and measured hydrocarbon IVOC concentration and SOA concentration at Pasadena, CA (Hayes et al., 2013; Zhao et al., 2014). Since there are limited data on

https://doi.org/10.5194/acp-2019-986
Preprint. Discussion started: 30 October 2019


Atmospheric Chemistry and Physics Discussions

non-mobile IVOC emissions, they are assumed to have the same properties as alkane-like IVOCs (IVOCP6-ALK to IVOCP3-ALK) with a uniform volatility distribution. Table 4 shows that Case 3 and 4 adds an average 30.7 and 68.5 Ton per day non-mobile IVOC emissions scaled from NMOG emissions as described in Section 3.4.

For Case 3 (Low nonmobile-IVOC) we added non-mobile IVOC emissions equivalent to 12% non-mobile NMOG emission. The scaling coefficient is determined to roughly match the campaign-average hydrocarbon IVOC mass concentrations measured in Pasadena, CA (Zhao et al., 2014). The only difference between Cases 2 and 3 are additional non-mobile hydrocarbon IVOC emissions.

The high nonmobile-IVOC case (Case 4) adds non-mobile IVOC emissions equivalent to 26.8% of non-mobile NMOG emissions. This value was chosen to roughly close the mildly-oxygenated IVOC and SOA mass balance. It is obviously a very high estimate, but only somewhat higher than the 20% estimates of total VCP emissions in McDonald et al. (2018). The difference between cases (4) and (3) is more additional non-mobile IVOC emissions equivalent to 14.8% of NMOG.

Figure 3(b) shows in Case 3, the model predicts 4.9 μg m^{-3} of nonmobile hydrocarbon IVOC and 7.3 μg m^{-3} of total hydrocarbon IVOC, which is only somewhat higher than the measured value (6.3 μg m^{-3}). Case 4 predicts additional 6.3 μg m^{-3} of oxygenated IVOC from non-mobile sources and 13.6 μg m^{-3} total IVOC (hydrocarbon + oxygenated), which exceeds the measured total IVOC (10.5 μg m^{-3}) by 30%. Given this overprediction and the fact that mildly-oxygenated IVOCs can also be formed through secondary chemistry, the IVOC-to-NMOG ratio for non-mobile sources needs to be between Case 3 (12%) and Case 4 (26.8%). In addition, recent research suggests that a factor of 3 scale-up is needed for VCP NMOG emissions, which would drive down the IVOC-to-NMOG ratios to 4 - 9% (McDonald et al., 2018).

4.2.2 OA time series and SOA/POA diurnal patterns

Adding non-mobile IVOC emissions, Cases 3 and 4 increased the afternoon peak SOA concentration to 4.98 and 8.56 μg m^{-3}, respectively. This highlights the potential important contribution of non-mobile emissions to SOA formation. Figure 5(a) also shows that in Case 4, modelled OA time series explains the measured SOA (RMSE = 2.5 μg m^{-3}, r = 0.85), including the peak values in the middle of the days. Since higher IVOC emissions also shifts the gas-particle partition equilibrium to the particle phase (Donahue et al., 2006), there are also minor differences in POA partitioning from Case 1 to Case 4, but these changes are relatively small and the measured and modelled POA agree (Figure 5c).

Non-mobile IVOC emissions also improve the modelled predictions of SOA contribution to OA in Pasadena. Hayes et al. (2013) reported 66% of OA as OOA (SV-OOA + LV-OOA) in Pasadena during CalNex campaign. Hersey et al. (2011) reported an even higher fraction of 77% OA as OOA in Pasadena in 2009. As a comparison, if no IVOCs are modelled, Case 1 only predicted 47%. With additional mobile and non-mobile IVOC emissions, our model predicts 67% OA as SOA in Case 3, and 74% in Case 4.

Although Case 4 reproduces the measured OA, increasing the IVOC emissions are likely not the only explanation. The assumption of Case 4 that non-mobile IVOC emission rate as 26.8% NMOG is likely too high, and it overpredicts the total IVOC concentrations. Other explanations that could improve SOA prediction includes (1) effect of vapor wall loss on

https://doi.org/10.5194/acp-2019-986
Preprint. Discussion started: 30 October 2019


Atmospheric Chemistry and Physics Discussions

SOA yield, (2) PBL modelling and (3) SOA aging. First, SOA yields for VOCs and IVOCs need to be corrected (typically increased) for vapor wall-losses (Akherati et al., 2018; Zhang et al., 2014). Second, CMAQ likely overpredicts the afternoon PBL height in Pasadena, as discussed in section 4.1. Correcting this issue will reduce the amount of IVOC emissions needed to reach SOA mass closure. Finally, the effects of aging on secondary products of SOA precursor oxidation is uncertain. We have represented this phenomenon with model parameters designed for aging of SVOC emissions (Murphy et al., 2017), but the ratio of functionalization versus fragmentation could be different for products of IVOC oxidation due to differences in carbon number and functionality.

Despite all of the uncertainties, the exploratory simulations (Cases 3 and 4) indicate non-mobile IVOC emissions are likely an important source of SOA precursors, but its contributions should be between Case 3 and 4 (12% and 26.8% of non-mobile NMOG). The lower value will close the hydrocarbon IVOC but not the SOA mass balance, which are influenced by other factors such as biased yields due to wall losses. Again, the likely underrepresentation of VCP emissions (McDonald et al., 2018) in current inventories will drive down the needed non-mobile IVOC emissions to be 4% to 9% of NMOG emissions.

4.3 IVOCs and regional SOA formation

IVOCs also contribute to regional SOA formation. This is shown in Figure 6 (a, b), which presents maps of campaign-average NMOG emission and modelled SOA concentration in California. Primary emissions are concentrated in heavily populated urban areas such as Los Angeles. However, due to the regional transport of SOA precursors, especially IVOCs, Figure 6(b) shows the predicted SOA is spread over a much large spatial domain. This is expected given the SOA production depends on atmospheric oxidation.

To examine the spatial performance of the model, we also compared our model-predictions of regional OA using the CSN data at seven sites in California. Figure 6(c) shows the location of the CSN sites. Three of the sites are in southern California (LA, Riverside and El Cajon) while the others are central or northern California. Figure 6(d) shows the comparison between modelled OA and CSN data (OC*1.8) for all seven sites from Case 1 to Case 4. Table 5 summarizes the evaluation metrics for all cases in site-aggregated comparisons.

Case 1 grossly underestimated OA at all sites except for Sacramento, with an fractional bias (FB, $\frac{1}{N}\sum_{i=1}^{N}\frac{P-M}{\frac{P+M}{2}}$, P is the predicted value, M is the measured value, and N is the sample size) of -0.59 and fractional error (FE, $\frac{1}{N}\sum_{i=1}^{N}\frac{|P-M|}{\frac{P+M}{2}}$) of 0.67, of which much of the measured OA are SOA (Docherty et al., 2008; Hayes et al., 2013). Case 2 and Case 3 reduce the fractional bias to -0.52 and -0.33, respectively, and the Fractional Error to 0.62 to 0.49. Figure 6(d) shows that Case 3 best predicts OA concentrations across the southern California sites, but underpredicts other sites such as Fresno, San Jose and Bakersfield. Case 4 overpredicts the OA concentrations at the southern California CSN sites like LA, Riverside and El

https://doi.org/10.5194/acp-2019-986
Preprint. Discussion started: 30 October 2019


Atmospheric Chemistry and Physics Discussions

Cajon, but still underpredicts OA in Bakersfield, San Jose and Fresno. however, this case has the best overall metrics (FB = -0.10 and FE = 0.42).

Figure 6(b) shows that from Case 1 to Case 4, the amount of SOA formed from additional IVOC emissions is much less in northern and central California compared to southern California. This could be due to the different meteorological conditions or sources variations. Case 3 and Case 4 were estimated to roughly explain the measured hydrocarbon IVOC and SOA concentration in Pasadena, but source-specific IVOC-to-NMOG fractions are needed to correctly model the non-mobile emissions spatially.

5 Conclusions

This paper presents both the use of new mobile-source emission volatility profiles and a new SOA parameterization for mobile source IVOCs implementation in CTMs. The study then quantifies the effect of IVOC emissions from mobile and non-mobile anthropogenic sources to the IVOC ambient concentration and SOA formation in California during the CalNex campaign. Our approach may be applied to other sectors of organic combustion in the future, such as wildfires, agricultural fires, and meat cooking. The main findings are:

(1) We developed a new parameterization to model SOA formation from mobile source IVOC emissions. This required six lumped SOA precursor species to account for the differences in both volatility and chemical composition across mobile sources IVOC emissions. The lumped species were distributed in both volatility and chemical space. Two of the species are modelled using aromatic surrogates and the other four with aliphatic surrogates. New IVOC species and related profiles are available in SPECIATE 5.0 to facilitate their use in other CTM studies.

(2) We implemented comprehensive mobile IVOC emission profiles based on direct measurements. Mobile sources are predicted to contribute 2.4 μg m^{-3} of hydrocarbon IVOCs at Pasadena site during CalNex, which is 38% of measured concentrations.

(3) Mobile IVOC emissions are predicted to contribute ~1 μg m^{-3} daily-average SOA concentration, a 67% increase compared to the base case without IVOC emissions. Therefore, these emissions need to be routinely included in CTM simulations. But mobile source emissions alone don't explain measured IVOC or SOA concentration. This underscores effectiveness of decades of increasingly effective mobile source emission standard. Other sources are becoming relatively more important in the NMOG and IVOC emission inventory in the South Coast.

(4) Our analysis suggests that 12% to 26.8% (or 30.7 to 68.5 Ton day^{-1} in Los Angeles – Pasadena region) of non-mobile NMOG emissions need to be IVOC to explain the measured hydrocarbon IVOCs and SOA formation. Modelled OA in high-non-mobile IVOC case (Case 4) explains AMS-measured OA values (RMSE = 2.5 μg m^{-3}, r = 0.85).

Future research and inventory needs include:

https://doi.org/10.5194/acp-2019-986
Preprint. Discussion started: 30 October 2019


Atmospheric Chemistry and Physics Discussions

(1) IVOC emissions from non-mobile sources are important. VCPs are likely a major contributor here and further research should seek to constrain emissions from these sources using ambient observations, bottom-up emission inventory methods and computational models (McDonald et al., 2018; Qin et al., 2019). Measurements of both volatility distribution as well as chemical composition are valuable. New chemical mechanism species for oxygenated IVOCs may also be needed.

(2) More measurements of ambient IVOC concentrations at different sites are needed to evaluate models. Our analysis suggests fitting IVOC-to-NMOG ratios at one site for non-mobile source is not enough to correctly model OA formation in California. Regional evaluations of ambient IVOC and OA predictions still have large uncertainty.

(3) Improved understanding of the effects of multi-day aging on SOA formed from IVOC emissions. The impacts of polluted plumes on downwind receptors depends on the nature of aging processes and whether they result in the addition or reduction of particulate mass (e.g. fragmentation processes may enhance volatilization of OA downwind of sources).

Disclaimer. Although portions of this work were contributed by research staff in the Environmental Protection Agency and this work has been reviewed and approved for publication, it does not reflect official policy of the EPA.

Author contributions

QL, BNM, ALR designed the research. QL, BNM, PJA, YZ and ALR designed the SOA formation parameterization from IVOCs and carried them out. QL, BNM, MQ, PJA, HOTP, CE, CA and ALR designed the CMAQ model configuration and simulations and carried them out. QL wrote the paper with inputs from all co-authors.

Acknowledgment

This publication was developed as part of the Center for Air, Climate, and Energy Solutions (CACES), which is supported under Assistance Agreement No. RD83587301 awarded by the U.S. Environmental Protection Agency. This publication was also supported by Oak Ridge Institute for Science and Education (ORISE) Research Participation Program for the U.S. Environmental Protection Agency (EPA). The views expressed in this document are solely those of authors and do not necessarily reflect those of the Agency. EPA does not endorse any products or commercial services mentioned in this publication. The authors thank Dr. Neil Donahue for helpful discussions.

https://doi.org/10.5194/acp-2019-986
Preprint. Discussion started: 30 October 2019

Atmospheric Chemistry and Physics Discussions

References

Akherati, A., Cappa, C. D., Kleeman, M. J., Docherty, K. S., Jimenez, J. L., Griffith, S. M., Dusanter, S., Stevens, P. S. and Jathar, S. H.: Simulating secondary organic aerosol in a regional air quality model using the statistical oxidation model - Part 3: Assessing the influence of semi-volatile and intermediate volatility organic compounds and NOX, Atmos. Chem. Phys. Discuss., 2018, 1–44, doi:10.5194/acp-2018-616, 2018.

Apte, J. S., Brauer, M., Cohen, A. J., Ezzati, M. and Pope, C. A.: Ambient PM2.5 Reduces Global and Regional Life Expectancy, Environ. Sci. Technol. Lett., 5(9), 546–551, doi:10.1021/acs.estlett.8b00360, 2018.

Baker, K. R., Carlton, A. G., Kleindienst, T. E., Offenberg, J. H., Beaver, M. R., Gentner, D. R., Goldstein, A. H., Hayes, P. L., Jimenez, J. L., Gilman, J. B., De Gouw, J. A., Woody, M. C., Pye, H. O. T. T., Kelly, J. T., Lewandowski, M., Jaoui, M., Stevens, P. S., Brune, W. H., Lin, Y. H., Rubitschun, C. L. and Surratt, J. D.: Gas and aerosol carbon in California: Comparison of measurements and model predictions in Pasadena and Bakersfield, Atmos. Chem. Phys., 15(9), 5243–5258, doi:10.5194/acp-15-5243-2015, 2015.

Bash, J. O., Baker, K. R. and Beaver, M. R.: Evaluation of improved land use and canopy representation in BEIS v3.61 with biogenic VOC measurements in California, Geosci. Model Dev., 9(6), 2191–2207, doi:10.5194/gmd-9-2191-2016, 2016.

Borbon, A., Gilman, J. B., Kuster, W. C., Grand, N., Chevaillier, S., Colomb, A., Dolgorouky, C., Gros, V., Lopez, M., Sarda-Esteve, R., Holloway, J., Stutz, J., Petetin, H., McKeen, S., Beekmann, M., Warneke, C., Parrish, D. D. and De Gouw, J. A.: Emission ratios of anthropogenic volatile organic compounds in northern mid-latitude megacities: Observations versus emission inventories in Los Angeles and Paris, J. Geophys. Res. Atmos., 118(4), 2041–2057, doi:10.1002/jgrd.50059, 2013.

Carter, W. P. L.: Saprc-07 Chemical Mechanism, , (05), 2010.

Chan, A. W. H., Kautzman, K. E., Chhabra, P. S., Surratt, J. D., Chan, M. N., Crounse, J. D., Kürten, A., Wennberg, P. O., Flagan, R. C. and Seinfeld, J. H.: Secondary organic aerosol formation from photooxidation of naphthalene and alkylnaphthalenes: Implications for oxidation of intermediate volatility organic compounds (IVOCs), Atmos. Chem. Phys., 9(9), 3049–3060, doi:10.5194/acp-9-3049-2009, 2009.

Cross, E. S., Hunter, J. F., Carrasquillo, A. J., Franklin, J. P., Herndon, S. C., Jayne, J. T., Worsnop, D. R., Miake-Lye, R. C. and Kroll, J. H.: Online measurements of the emissions of intermediate-volatility and semi-volatile organic compounds from aircraft, Atmos. Chem. Phys., 13(15), 7845–7858, doi:10.5194/acp-13-7845-2013, 2013.

Cross, E. S., Sappok, A. G., Wong, V. W. and Kroll, J. H.: Load-Dependent Emission Factors and Chemical Characteristics of IVOCs from a Medium-Duty Diesel Engine, Environ. Sci. Technol., 49(22), 13483–13491, doi:10.1021/acs.est.5b03954, 2015.

Di, Q., Wang, Y., Zanobetti, A., Wang, Y., Koutrakis, P., Choirat, C., Dominici, F. and Schwartz, J. D.: Air Pollution and Mortality in the Medicare Population, N. Engl. J. Med., 376(26), 2513–2522, doi:10.1056/NEJMoa1702747, 2017.

Docherty, K. S., Stone, E. A., Ulbrich, I. M., DeCarlo, P. F., Snyder, D. C., Schauer, J. J., Peltier, R. E., Weber, R. J., Murphy, S. M. and Seinfeld, J. H.: Apportionment of primary and secondary organic aerosols in Southern California during

the 2005 Study of Organic Aerosols in Riverside (SOAR-1), Environ. Sci. Technol., 42(20), 7655–7662, 2008.

Donahue, N. M., Robinson, A. L., Stanier, C. O. and Pandis, S. N.: Coupled Partitioning, Dilution, and Chemical Aging of Semivolatile Organics, Environ. Sci. Technol., 40(8), 2635–2643, doi:10.1021/es052297c, 2006.

Drozd, G. T., Zhao, Y., Saliba, G., Frodin, B., Maddox, C., Oliver Chang, M.-C., Maldonado, H., Sardar, S., Weber, R. J., Robinson, A. L. and Goldstein, A. H.: Detailed Speciation of Intermediate Volatility and Semivolatile Organic Compound Emissions from Gasoline Vehicles: Effects of Cold-Starts and Implications for Secondary Organic Aerosol Formation, Environ. Sci. Technol., 53(3), 1706–1714, doi:10.1021/acs.est.8b05600, 2019.

Ensberg, J. J., Hayes, P. L., Jimenez, J. L., Gilman, J. B., Kuster, W. C., De Gouw, J. A., Holloway, J. S., Gordon, T. D., Jathar, S., Robinson, A. L. and Seinfeld, J. H.: Emission factor ratios, SOA mass yields, and the impact of vehicular emissions on SOA formation, Atmos. Chem. Phys., 14(5), 2383–2397, doi:10.5194/acp-14-2383-2014, 2014.

Fast, J. D., Allan, J., Bahreini, R., Craven, J., Emmons, L., Ferrare, R., Hayes, P. L., Hodzic, A., Holloway, J., Hostetler, C., Jimenez, J. L., Jonsson, H., Liu, S., Liu, Y., Metcalf, A., Middlebrook, A., Nowak, J., Pekour, M., Perring, A., Russell, L., Sedlacek, A., Seinfeld, J., Setyan, A., Shilling, J., Shrivastava, M., Springston, S., Song, C., Subramanian, R., Taylor, J. W., Vinoj, V., Yang, Q., Zaveri, R. A. and Zhang, Q.: Modeling regional aerosol and aerosol precursor variability over California and its sensitivity to emissions and long-range transport during the 2010 CalNex and CARES campaigns, Atmos. Chem. Phys., 14(18), 10013–10060, doi:10.5194/acp-14-10013-2014, 2014.

Gentner, D. R., Jathar, S. H., Gordon, T. D., Bahreini, R., Day, D. A., El Haddad, I., Hayes, P. L., Pieber, S. M., Platt, S. M., de Gouw, J., Goldstein, A. H., Harley, R. A., Jimenez, J. L., Prévôt, A. S. H. and Robinson, A. L.: Review of Urban Secondary Organic Aerosol Formation from Gasoline and Diesel Motor Vehicle Emissions, Environ. Sci. Technol., acs.est.6b04509, doi:10.1021/acs.est.6b04509, 2017.

Gordon, T. D., Tkacik, D. S., Presto, A. A., Zhang, M. and Shantanu, H.: Primary Gas- and Particle-Phase Emissions and Secondary Organic Aerosol Production from Gasoline and Diesel Off-Road Engines, 2013.

Gordon, T. D., Presto, A. A., May, A. A., Nguyen, N. T., Lipsky, E. M., Donahue, N. M., Gutierrez, A., Zhang, M., Maddox, C., Rieger, P., Chattopadhyay, S., Maldonado, H., Maricq, M. M. and Robinson, A. L.: Secondary organic aerosol formation exceeds primary particulate matter emissions for light-duty gasoline vehicles, Atmos. Chem. Phys., 14(9), 4661–4678, doi:10.5194/acp-14-4661-2014, 2014.

de Gouw, J. A., Gilman, J. B., Kim, S.-W., Alvarez, S. L., Dusanter, S., Graus, M., Griffith, S. M., Isaacman-VanWertz, G., Kuster, W. C., Lefer, B. L., Lerner, B. M., McDonald, B. C., Rappenglück, B., Roberts, J. M., Stevens, P. S., Stutz, J., Thalman, R., Veres, P. R., Volkamer, R., Warneke, C., Washenfelder, R. A. and Young, C. J.: Chemistry of Volatile Organic Compounds in the Los Angeles Basin: Formation of Oxygenated Compounds and Determination of Emission Ratios, J. Geophys. Res. Atmos., 123(4), 2298–2319, doi:10.1002/2017JD027976, 2018.

Hatch, L. E., Yokelson, R. J., Stockwell, C. E., Veres, P. R., Simpson, I. J., Blake, D. R., Orlando, J. J. and Barsanti, K. C.: Multi-instrument comparison and compilation of non-methane organic gas emissions from biomass burning and implications for smoke-derived secondary organic aerosol precursors, Atmos. Chem. Phys., 17(2), 1471–1489, doi:10.5194/acp-17-1471-

2017, 2017.

Hayes, P. L., Ortega, A. M., Cubison, M. J., Froyd, K. D., Zhao, Y., Cliff, S. S., Hu, W. W., Toohey, D. W., Flynn, J. H., Lefer, B. L., Grossberg, N., Alvarez, S., Rappenglück, B., Taylor, J. W., Allan, J. D., Holloway, J. S., Gilman, J. B., Kuster, W. C., De Gouw, J. A., Massoli, P., Zhang, X., Liu, J., Weber, R. J., Corrigan, A. L., Russell, L. M., Isaacman, G., Worton, D. R., Kreisberg, N. M., Goldstein, A. H., Thalman, R., Waxman, E. M., Volkamer, R., Lin, Y. H., Surratt, J. D., Kleindienst, T. E., Offenberg, J. H., Dusanter, S., Griffith, S., Stevens, P. S., Brioude, J., Angevine, W. M. and Jimenez, J. L.: Organic aerosol composition and sources in Pasadena, California, during the 2010 CalNex campaign, J. Geophys. Res. Atmos., 118(16), 9233–9257, doi:10.1002/jgrd.50530, 2013.

Hayes, P. L., Carlton, a. G., Baker, K. R., Ahmadov, R., Washenfelder, R. A., Alvarez, S., Rappenglück, B., Gilman, J. B., Kuster, W. C., de Gouw, J. A., Zotter, P., Prévôt, a. S. H., Szidat, S., Kleindienst, T. E., Offenberg, J. H., Ma, P. K. and Jimenez, J. L.: Modeling the formation and aging of secondary organic aerosols in Los Angeles during CalNex 2010, Atmos. Chem. Phys., 15(10), 5773–5801, doi:10.5194/acp-15-5773-2015, 2015.

Hersey, S. P., Craven, J. S., Schilling, K. A., Metcalf, A. R., Sorooshian, A., Chan, M. N., Flagan, R. C. and Seinfeld, J. H.: The Pasadena Aerosol Characterization Observatory (PACO): chemical and physical analysis of the Western Los Angeles basin aerosol, Atmos. Chem. Phys., 11(15), 7417–7443, 2011.

Hodzic, A., Jimenez, J. L., Madronich, S., Canagaratna, M. R., Decarlo, P. F., Kleinman, L. and Fast, J.: Modeling organic aerosols in a megacity: Potential contribution of semi-volatile and intermediate volatility primary organic compounds to secondary organic aerosol formation, Atmos. Chem. Phys., 10(12), 5491–5514, doi:10.5194/acp-10-5491-2010, 2010.

Huang, C., Hu, Q., Li, Y., Tian, J., Ma, Y., Zhao, Y., Feng, J., An, J., Qiao, L., Wang, H., Jing, S., Huang, D., Lou, S., Zhou, M., Zhu, S., Tao, S. and Li, L.: Intermediate Volatility Organic Compound Emissions from a Large Cargo Vessel Operated under Real-World Conditions, Environ. Sci. Technol., 52(21), 12934–12942, doi:10.1021/acs.est.8b04418, 2018.

Hunter, J. F., Day, D. A., Palm, B. B., Yatavelli, R. L. N., Chan, A. W. H., Kaser, L., Cappellin, L., Hayes, P. L., Cross, E. S., Carrasquillo, A. J., Campuzano-Jost, P., Stark, H., Zhao, Y., Hohaus, T., Smith, J. N., Hansel, A., Karl, T., Goldstein, A. H., Guenther, A., Worsnop, D. R., Thornton, J. A., Heald, C. L., Jimenez, J. L. and Kroll, J. H.: Comprehensive characterization of atmospheric organic carbon at a forested site, Nat. Geosci., 10, 748 [online] Available from: http://dx.doi.org/10.1038/ngeo3018, 2017.

Hutzell, W. T., Luecken, D. J., Appel, K. W. and Carter, W. P. L.: Interpreting predictions from the SAPRC07 mechanism based on regional and continental simulations, Atmos. Environ., 46, 417–429, doi:https://doi.org/10.1016/j.atmosenv.2011.09.030, 2012.

Jathar, S. H., Miracolo, M. A., Tkacik, D. S., Donahue, N. M., Adams, P. J. and Robinson, A. L.: Secondary organic aerosol formation from photo-oxidation of unburned fuel: experimental results and implications for aerosol formation from combustion emissions., Environ. Sci. Technol., 47(22), 12886–93, doi:10.1021/es403445q, 2013.

Jathar, S. H., Woody, M., Pye, H. O. T., Baker, K. R. and Robinson, A. L.: Chemical transport model simulations of organic aerosol in southern California: model evaluation and gasoline and diesel source contributions, Atmos. Chem. Phys., 17(6),

4305–4318, doi:10.5194/acp-17-4305-2017, 2017.

Jimenez, J. L., Canagaratna, M. R., Donahue, N. M., Prevot, A. S. H., Zhang, Q., Kroll, J. H., DeCarlo, P. F., Allan, J. D., Coe, H., Ng, N. L., Aiken, A. C., Docherty, K. S., Ulbrich, I. M., Grieshop, A. P., Robinson, A. L., Duplissy, J., Smith, J. D., Wilson, K. R., Lanz, V. A., Hueglin, C., Sun, Y. L., Tian, J., Laaksonen, A., Raatikainen, T., Rautiainen, J., Vaattovaara, P., Ehn, M., Kulmala, M., Tomlinson, J. M., Collins, D. R., Cubison, M. J., Dunlea, J., Huffman, J. A., Onasch, T. B., Alfarra, M. R., Williams, P. I., Bower, K., Kondo, Y., Schneider, J., Drewnick, F., Borrmann, S., Weimer, S., Demerjian, K., Salcedo, D., Cottrell, L., Griffin, R., Takami, A., Miyoshi, T., Hatakeyama, S., Shimono, A., Sun, J. Y., Zhang, Y. M., Dzepina, K., Kimmel, J. R., Sueper, D., Jayne, J. T., Herndon, S. C., Trimborn, A. M., Williams, L. R., Wood, E. C., Middlebrook, A. M., Kolb, C. E., Baltensperger, U. and Worsnop, D. R.: Evolution of Organic Aerosols in the Atmosphere, Science (80-.)., 326(5959), 1525–1529 [online] Available from: http://science.sciencemag.org/content/326/5959/1525.abstract, 2009.

Khare, P. and Gentner, D. R.: Considering the future of anthropogenic gas-phase organic compound emissions and the increasing influence of non-combustion sources on urban air quality, Atmos. Chem. Phys., 18(8), 5391–5413, doi:10.5194/acp-18-5391-2018, 2018.

Kim, S.-W., McDonald, B. C., Baidar, S., Brown, S. S., Dube, B., Ferrare, R. A., Frost, G. J., Harley, R. A., Holloway, J. S., Lee, H.-J., McKeen, S. A., Neuman, J. A., Nowak, J. B., Oetjen, H., Ortega, I., Pollack, I. B., Roberts, J. M., Ryerson, T. B., Scarino, A. J., Senff, C. J., Thalman, R., Trainer, M., Volkamer, R., Wagner, N., Washenfelder, R. A., Waxman, E. and Young, C. J.: Modeling the weekly cycle of NOx and CO emissions and their impacts on O3 in the Los Angeles-South Coast Air Basin during the CalNex 2010 field campaign, J. Geophys. Res. Atmos., 121(3), 1340–1360, doi:10.1002/2015JD024292, 2016.

Koo, B., Knipping, E. and Yarwood, G.: 1.5-Dimensional volatility basis set approach for modeling organic aerosol in CAMx and CMAQ, Atmos. Environ., 95, 158–164, doi:10.1016/j.atmosenv.2014.06.031, 2014.

Kroll, J. H., Cross, E. S., Hunter, J. F., Carrasquillo, A. J., Franklin, J. P., Herndon, S. C., Jayne, J. T., Worsnop, D. R., Lye, R. C. M. and Onasch, T. B.: Emissions of Gas - Phase Low - Volatility Organic Compounds from Mobile Sources, , (March), 2014.

Liggio, J., Li, S., Hayden, K., Taha, Y. M., Stroud, C., Darlington, A., Drollette, B. D., Gordon, M., Lee, P., Liu, P., Leithead, A., Moussa, S. G., Wang, D., Brien, J. O., Mittermeier, R. L., Osthoff, H. D., Makar, P. A., Zhang, J., Brook, J. R., Lu, G., Staebler, R. M., Han, Y., Travis, W., Plata, D. L. and Gentner, D. R.: Oil sands operations as a large source of secondary organic aerosols, Nature, 534(7605), 1–16, doi:10.1038/nature17646, 2016.

Lim, Y. Bin and Ziemann, P. J.: Products and mechanism of secondary organic aerosol formation from reactions of n-alkanes with OH radicals in the presence of NO x, Environ. Sci. Technol., 39(23), 9229–9236, 2005.

Lim, Y. Bin and Ziemann, P. J.: Chemistry of Secondary Organic Aerosol Formation from OH Radical-Initiated Reactions of Linear, Branched, and Cyclic Alkanes in the Presence of NO x , Aerosol Sci. Technol., 43(6), 604–619, doi:10.1080/02786820902802567, 2009.

Lu, Q., Zhao, Y. and Robinson, A. L.: Comprehensive organic emission profiles for gasoline, diesel, and gas-turbine engines including intermediate and semi-volatile organic compound emissions, Atmos. Chem. Phys. Discuss., 2018, 1–28, doi:10.5194/acp-2018-752, 2018.

May, A. A., Presto, A. A., Hennigan, C. J., Nguyen, N. T., Gordon, T. D. and Robinson, A. L.: Gas-particle partitioning of primary organic aerosol emissions: (2) diesel vehicles, Environ. Sci. Technol., 47(15), 8288–8296, doi:10.1021/es400782j, 2013a.

May, A. A., Levin, E. J. T., Hennigan, C. J., Riipinen, I., Lee, T., Collett, J. L., Jimenez, J. L., Kreidenweis, S. M. and Robinson, A. L.: Gas-particle partitioning of primary organic aerosol emissions: 3. Biomass burning, J. Geophys. Res. Atmos., 118(19), 11327–11338, doi:10.1002/jgrd.50828, 2013b.

May, A. A., Nguyen, N. T., Presto, A. A., Gordon, T. D., Lipsky, E. M., Karve, M., Gutierrez, A., Robertson, W. H., Zhang, M., Brandow, C., Chang, O., Chen, S., Cicero-Fernandez, P., Dinkins, L., Fuentes, M., Huang, S. M., Ling, R., Long, J., Maddox, C., Massetti, J., McCauley, E., Miguel, A., Na, K., Ong, R., Pang, Y., Rieger, P., Sax, T., Truong, T., Vo, T., Chattopadhyay, S., Maldonado, H., Maricq, M. M. and Robinson, A. L.: Gas- and particle-phase primary emissions from in-use, on-road gasoline and diesel vehicles, Atmos. Environ., 88, 247–260, doi:10.1016/j.atmosenv.2014.01.046, 2014.

McDonald, B. C., de Gouw, J. A., Gilman, J. B., Jathar, S. H., Akherati, A., Cappa, C. D., Jimenez, J. L., Lee-Taylor, J., Hayes, P. L., McKeen, S. A., Cui, Y. Y., Kim, S.-W., Gentner, D. R., Isaacman-VanWertz, G., Goldstein, A. H., Harley, R. A., Frost, G. J., Roberts, J. M., Ryerson, T. B. and Trainer, M.: Volatile chemical products emerging as largest petrochemical source of urban organic emissions, Science (80-.)., 359(6377), 760–764, doi:10.1126/science.aaq0524, 2018.

Miracolo, M. A., Hennigan, C. J., Ranjan, M., Nguyen, N. T., Gordon, T. D., Lipsky, E. M., Presto, A. A., Donahue, N. M. and Robinson, A. L.: Secondary aerosol formation from photochemical aging of aircraft exhaust in a smog chamber, Atmos. Chem. Phys., 11(9), 4135–4147, 2011.

Murphy, B. N., Woody, M. C., Jimenez, J. L., Carlton, A. M. G., Hayes, P. L., Liu, S., Ng, N. L., Russell, L. M., Setyan, A., Xu, L., Young, J., Zaveri, R. A., Zhang, Q. and Pye, H. O. T.: Semivolatile POA and parameterized total combustion SOA in CMAQv5.2: Impacts on source strength and partitioning, Atmos. Chem. Phys., 17(18), 11107–11133, doi:10.5194/acp-17-11107-2017, 2017.

Pereira, K. L., Dunmore, R., Whitehead, J., Alfarra, M. R., Allan, J. D., Alam, M. S., Harrison, R. M., McFiggans, G. and Hamilton, J. F.: Technical note: Use of an atmospheric simulation chamber to investigate the effect of different engine conditions on unregulated VOC-IVOC diesel exhaust emissions, Atmos. Chem. Phys., 18(15), 11073–11096, doi:10.5194/acp-18-11073-2018, 2018.

Platt, S. M., El Haddad, I., Pieber, S. M., Zardini, A. A., Suarez-Bertoa, R., Clairotte, M., Daellenbach, K. R., Huang, R.-J., Slowik, J. G., Hellebust, S., Temime-Roussel, B., Marchand, N., de Gouw, J., Jimenez, J. L., Hayes, P. L., Robinson, A. L., Baltensperger, U., Astorga, C. and Prévôt, A. S. H.: Gasoline cars produce more carbonaceous particulate matter than modern filter-equipped diesel cars, Sci. Rep., 7(1), 4926, doi:10.1038/s41598-017-03714-9, 2017.

Presto, A. A., Miracolo, M. A., Kroll, J. H., Worsnop, D. R., Robinson, A. L. and Donahue, N. M.: Intermediate-volatility

organic compounds: A potential source of ambient oxidized organic aerosol, Environ. Sci. Technol., 43(13), 4744–4749, doi:10.1021/es803219q, 2009.

Presto, A. A., Miracolo, M. A., Donahue, N. M. and Robinson, A. L.: Secondary Organic Aerosol Formation from High-NOx Photo-Oxidation of Low Volatility Precursors: n-Alkanes, Environ. Sci. Technol., 44(6), 2029–2034, doi:10.1021/es903712r, 2010a.

Presto, A. A., Nguyen, N. T., Ranjan, M., Reeder, A. J., Lipsky, E. M., Hennigan, C. J., Miracolo, M. A., Riemer, D. D. and Robinson, A. L.: Fine particle and organic vapor emissions from staged tests of an in-use aircraft engine, Atmos. Environ., 45(21), 3603–3612, doi:10.1016/j.atmosenv.2011.03.061, 2011.

Presto, A. a, Miracolo, M. a, Donahue, N. M. and Robinson, A. L.: Secondary Organic Aerosol Formation from High-NO x Photo-Oxidation of Low Volatility Precursors : n -Alkanes, Atmos. Chem. Phys., 44(6), 2029–2034, 2010b.

Pye, H. O. T., Murphy, B. N., Xu, L., Ng, N. L., Carlton, A. G., Guo, H., Weber, R., Vasilakos, P., Appel, K. W., Budisulistiorini, S. H., Surratt, J. D., Nenes, A., Hu, W., Jimenez, J. L., Isaacman-VanWertz, G., Misztal, P. K. and Goldstein, A. H.: On the implications of aerosol liquid water and phase separation for organic aerosol mass, Atmos. Chem. Phys., 17(1), 343–369, doi:10.5194/acp-17-343-2017, 2017.

Qin, M., Murphy, B. N., McDonald, B. C. B., McKeen, S. A., Koval, L. and al, et: Impacts of volatile chemical products on criteria pollutants in an urban atmosphere (in preparation), 2019.

Ranjan, M., Presto, A. a., May, A. a. and Robinson, A. L.: Temperature Dependence of Gas–Particle Partitioning of Primary Organic Aerosol Emissions from a Small Diesel Engine, Aerosol Sci. Technol., 46(1), 13–21, doi:10.1080/02786826.2011.602761, 2012.

Ryerson, T. B., Andrews, A. E., Angevine, W. M., Bates, T. S., Brock, C. A., Cairns, B., Cohen, R. C., Cooper, O. R., de Gouw, J. A., Fehsenfeld, F. C., Ferrare, R. A., Fischer, M. L., Flagan, R. C., Goldstein, A. H., Hair, J. W., Hardesty, R. M., Hostetler, C. A., Jimenez, J. L., Langford, A. O., McCauley, E., McKeen, S. A., Molina, L. T., Nenes, A., Oltmans, S. J., Parrish, D. D., Pederson, J. R., Pierce, R. B., Prather, K., Quinn, P. K., Seinfeld, J. H., Senff, C. J., Sorooshian, A., Stutz, J., Surratt, J. D., Trainer, M., Volkamer, R., Williams, E. J. and Wofsy, S. C.: The 2010 California Research at the Nexus of Air Quality and Climate Change (CalNex) field study, J. Geophys. Res. Atmos., 118(11), 5830–5866, doi:10.1002/jgrd.50331, 2013.

Skamarock, W. C., Klemp, J. B., Dudhia, J., Gill, D. O., Barker, D. M., Duda, M. G., Huang, X.-Y., Wang, W. and Powers, J. G.: A Description of the Advanced Research WRF Version 3, 2008.

Subramanian, R., Khlystov, A. Y., Cabada, J. C. and Robinson, A. L.: Positive and Negative Artifacts in Particulate Organic Carbon Measurements with Denuded and Undenuded Sampler Configurations Special Issue of Aerosol Science and Technology on Findings from the Fine Particulate Matter Supersites Program, Aerosol Sci. Technol., 38(sup1), 27–48, doi:10.1080/02786820390229354, 2004.

Tkacik, D. S., Presto, A. A., Donahue, N. M. and Robinson, A. L.: Secondary organic aerosol formation from intermediate-volatility organic compounds: Cyclic, linear, and branched alkanes, Environ. Sci. Technol., 46(16), 8773–8781,

doi:10.1021/es301112c, 2012.

US EPA: Final Report, SPECIATE Version 5.0, Database Development Documentation. [online] Available from: https://www.epa.gov/sites/production/files/2019-07/documents/speciate_5.0.pdf, 2019.

USEPA: MOVES 2014a, [online] Available from: https://www.epa.gov/moves/moves2014a-latest-version-motor-vehicle-emission-simulator-moves#manuals, 2014.

Wang, X., Cheung, C. S., Di, Y. and Huang, Z.: Diesel engine gaseous and particle emissions fueled with diesel-oxygenate blends, Fuel, 94, 317–323, doi:10.1016/j.fuel.2011.09.016, 2012.

Warneke, C., de Gouw, J. A., Holloway, J. S., Peischl, J., Ryerson, T. B., Atlas, E., Blake, D., Trainer, M. and Parrish, D. D.: Multiyear trends in volatile organic compounds in Los Angeles, California: Five decades of decreasing emissions, J. Geophys. Res. Atmos., 117(D21), doi:10.1029/2012JD017899, 2012.

Woody, M. C., Baker, K. R., Hayes, P. L., Jimenez, J. L., Koo, B. and Pye, H. O. T. T.: Understanding sources of organic aerosol during CalNex-2010 using the CMAQ-VBS, Atmos. Chem. Phys., 16(6), 4081–4100, doi:10.5194/acp-16-4081-2016, 2016.

Worton, D. R., Isaacman, G., Gentner, D. R., Dallmann, T. R., Chan, A. W. H., Ruehl, C., Kirchstetter, T. W., Wilson, K. R., Harley, R. A. and Goldstein, A. H.: Lubricating Oil Dominates Primary Organic Aerosol Emissions from Motor Vehicles, Environ. Sci. Technol., 48(7), 3698–3706, doi:10.1021/es405375j, 2014.

Xie, Y., Paulot, F., Carter, W. P. L., Nolte, C. G., Luecken, D. J., Hutzell, W. T., Wennberg, P. O., Cohen, R. C. and Pinder, R. W.: Understanding the impact of recent advances in isoprene photooxidation on simulations of regional air quality, Atmos. Chem. Phys., 13(16), 8439–8455, doi:10.5194/acp-13-8439-2013, 2013.

Xu, L., Pye, H. O. T., He, J., Chen, Y., Murphy, B. N. and Ng, N. L.: Experimental and model estimates of the contributions from biogenic monoterpenes and sesquiterpenes to secondary organic aerosol in the southeastern United States, Atmos. Chem. Phys., 18(17), 12613–12637, doi:10.5194/acp-18-12613-2018, 2018.

Zhang, R., Wang, G., Guo, S., Zamora, M. L., Ying, Q., Lin, Y., Wang, W., Hu, M. and Wang, Y.: Formation of Urban Fine Particulate Matter, Chem. Rev., 115(10), 3803–3855, doi:10.1021/acs.chemrev.5b00067, 2015.

Zhang, X., Cappa, C. D., Jathar, S. H., McVay, R. C., Ensberg, J. J., Kleeman, M. J., Seinfeld, J. H. and Christopher D. Cappa: Influence of vapor wall loss in laboratory chambers on yields of secondary organic aerosol., Proc. Natl. Acad. Sci. U. S. A., 111(16), 1–6, doi:10.1073/pnas.1404727111, 2014.

Zhang, Y., West, J. J., Mathur, R., Xing, J., Hogrefe, C., Roselle, S. J., Bash, J. O., Pleim, J. E., Gan, C.-M. and Wong, D. C.: Long-term trends in the ambient PM2.5- and O3-related mortality burdens in the United States under emission reductions from 1990 to 2010, Atmos. Chem. Phys., 18(20), 15003–15016, doi:10.5194/acp-18-15003-2018, 2018.

Zhao, Y., Hennigan, C. J., May, A. A., Tkacik, D. S., De Gouw, J. A., Gilman, J. B., Kuster, W. C., Borbon, A. and Robinson, A. L.: Intermediate-volatility organic compounds: A large source of secondary organic aerosol, Environ. Sci. Technol., 48(23), 13743–13750, doi:10.1021/es5035188, 2014.

Zhao, Y., Nguyen, N. T., Presto, A. A., Hennigan, C. J., May, A. A. and Robinson, A. L.: Intermediate Volatility Organic

https://doi.org/10.5194/acp-2019-986
Preprint. Discussion started: 30 October 2019

Atmospheric Chemistry and Physics Discussions

Compound Emissions from On-Road Diesel Vehicles: Chemical Composition, Emission Factors, and Estimated Secondary Organic Aerosol Production, Environ. Sci. Technol., 49(19), 11516–11526, doi:10.1021/acs.est.5b02841, 2015.

Zhao, Y., Nguyen, N. T., Presto, A. A., Hennigan, C. J., May, A. A. and Robinson, A. L.: Intermediate Volatility Organic Compound Emissions from On-Road Gasoline Vehicles and Small Off-Road Gasoline Engines, Environ. Sci. Technol., 50(8), 4554–4563, doi:10.1021/acs.est.5b06247, 2016.

Zhao, Y., Saleh, R., Saliba, G., Presto, A. A., Gordon, T. D., Drozd, G. T., Goldstein, A. H., Donahue, N. M. and Robinson, A. L.: Reducing secondary organic aerosol formation from gasoline vehicle exhaust, Proc. Natl. Acad. Sci. , 114(27), 6984–6989, doi:10.1073/pnas.1620911114, 2017.

Zhao, Y., Lambe, A. T., Saleh, R., Saliba, G. and Robinson, A. L.: Secondary Organic Aerosol Production from Gasoline Vehicle Exhaust: Effects of Engine Technology, Cold Start, and Emission Certification Standard, Environ. Sci. Technol., 52(3), 1253–1261, doi:10.1021/acs.est.7b05045, 2018.

https://doi.org/10.5194/acp-2019-986
Preprint. Discussion started: 30 October 2019

Atmospheric Chemistry and Physics Discussions

Tables

Table 1 Mass fractions (g per g NMOG) of IVOCs in mobile NMOG emission profiles used in CMAQ simulations

Group		Volatility (C*, µg m^{-3})	Source		
			Gasoline	Aircraft	Diesel
Non-aromatics	IVOCP6-ALK	10^6	0.006	0.207	0.159
	IVOCP5-ALK	10^5	0.002	0.048	0.187
	IVOCP4-ALK	10^4	0.003	0.020	0.149
	IVOCP3-ALK	10^3	0.003	0.009	0.054
Aromatics	IVOCP6-ARO	10^6	0.025	n/a	0.002
	IVOCP5-ARO	10^5	0.006	n/a	0.004
Total			0.046	0.285	0.555

https://doi.org/10.5194/acp-2019-986
Preprint. Discussion started: 30 October 2019

Atmospheric Chemistry and Physics Discussions

Table 2 Properties and SOA yields used for 6-group parameterization in CMAQ simulation

Group	C* ($\mu g\ m^{-3}$)	MW (g/mol)	$k_{OH} \times 10^{11}$ ($cm^{-1}\ molec^{-1}\ s^{-1}$)	α_i (C* = 0.1 – 100 $\mu g\ m^{-3}$)				Yield at 10 $\mu g\ m^{-3}$	H_{vap} ($kJ\ mol^{-1}$)
				0.1	1	10	100		
IVOCP6-ALK	10^6	184.4	1.55	0.009	0.045	0.118	0.470	0.15	19
IVOCP5-ALK	10^5	219.4	1.89	0.051	0.061	0.394	0.494	0.35	30
IVOCP4-ALK	10^4	254.9	2.25	0.068	0.083	0.523	0.239	0.43	41
IVOCP3-ALK	10^3	296.6	2.65	0.067	0.086	0.544	0.198	0.43	52
IVOCP6-ARO	10^6	162.3	3.05	0.022	0.109	0.251	0.005	0.25	19
IVOCP5-ARO	10^5	197.3	7.56	0.143	0.021	0.329	0.358	0.36	30

775

https://doi.org/10.5194/acp-2019-986
Preprint. Discussion started: 30 October 2019

Atmospheric Chemistry and Physics Discussions

Table 3 POA volatility distribution and filter artifact scaling factor used in CMAQ simulation

Source	Volatility, C* (μg m^{-3})				Filter artifact correction factor
	$\leq 10^{-1}$	1	10	10^{2}	
Gasoline	0.16	0.08	0.37	0.39	1.4
Diesel	0.21	0.11	0.33	0.36	1
Gas-turbine	0.15	0.26	0.38	0.21	1

https://doi.org/10.5194/acp-2019-986
Preprint. Discussion started: 30 October 2019

Atmospheric Chemistry and Physics Discussions

Table 4 Total anthropogenic organic emissions (Ton per day) in Los Angeles Basin region in four cases in this study

Case	Name	Traditional POA	POA after scaling	Traditional NMOG	Mobile IVOCs	Non-mobile IVOCs
1	Base	26.4	28.9	450.2	0	0
2	Mobile IVOC	26.4	28.9	450.2	27.6	0
3	Non-mobile low-IVOC	26.4	28.9	450.2	27.6	30.7
4	Non-mobile high-IVOC	26.4	28.9	450.2	27.6	68.5

780

https://doi.org/10.5194/acp-2019-986
Preprint. Discussion started: 30 October 2019

Atmospheric Chemistry and Physics Discussions

Table 5 Model OA performance metrics at all CSN sites (1.8*OC) for this study

Case	Fractional Bias	Fractional Error
1 Baseline	-0.59	0.67
2 Mobile-IVOC	-0.52	0.62
3 Low Non-mobile-IVOC	-0.33	0.49
4 High Non-mobile-IVOC	-0.10	0.42

https://doi.org/10.5194/acp-2019-986
Preprint. Discussion started: 30 October 2019

Atmospheric Chemistry and Physics Discussions

785 **Figures**

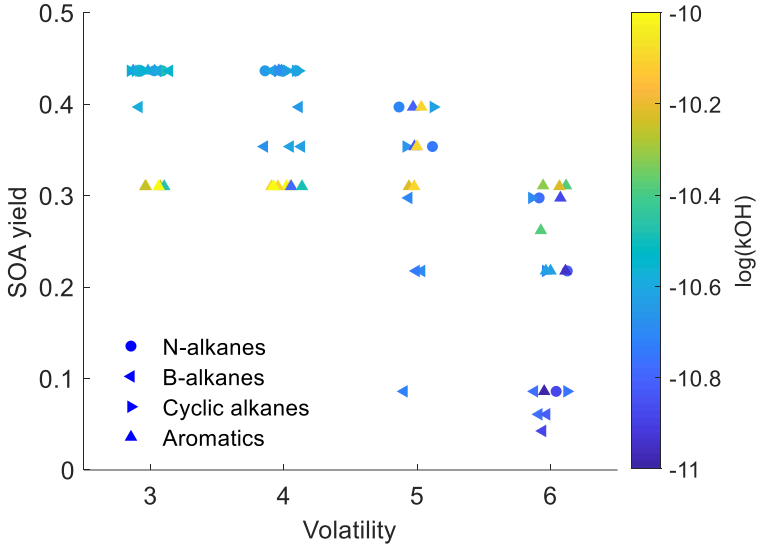

Figure 1: Scatter plot of first-generation SOA yields versus volatility in the detailed parameterization (dots are colored by OH reaction rates)

https://doi.org/10.5194/acp-2019-986
Preprint. Discussion started: 30 October 2019

Atmospheric Chemistry and Physics Discussions

790

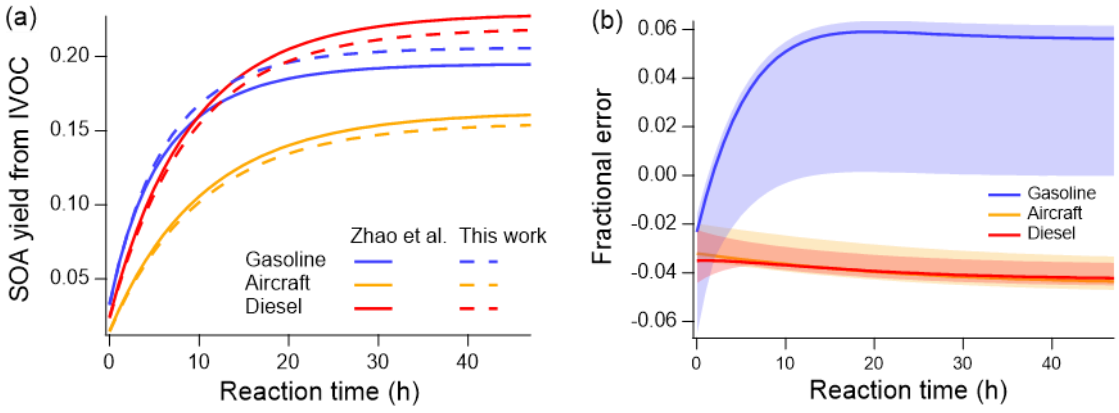

Figure 2: (a) Comparison of predicted SOA formation per unit mass mobile IVOC emission using original and reduced parameterizations at OA = 5 μg m^{-3}, average [OH] = 3 × 10^6 cm^{-3}. (b) Relative error in SOA formed between original and reduced parameterizations (Solid line is the relative error at OA = 5 μg m^{-3}, shaded area corresponds to OA = 1 to 50 μg m^{-3}).

795

https://doi.org/10.5194/acp-2019-986
Preprint. Discussion started: 30 October 2019

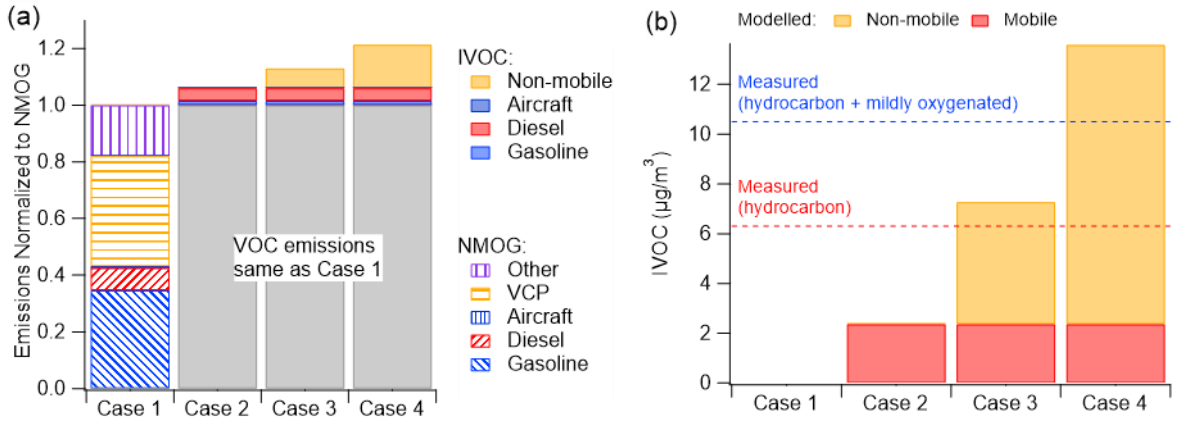

Figure 3: (a) Modelled NMOG and IVOC emissions by source for the four simulation cases. (b) Measured and modelled IVOC mass concentrations at Pasadena, CA during CalNex for the four simulation cases.

https://doi.org/10.5194/acp-2019-986
Preprint. Discussion started: 30 October 2019

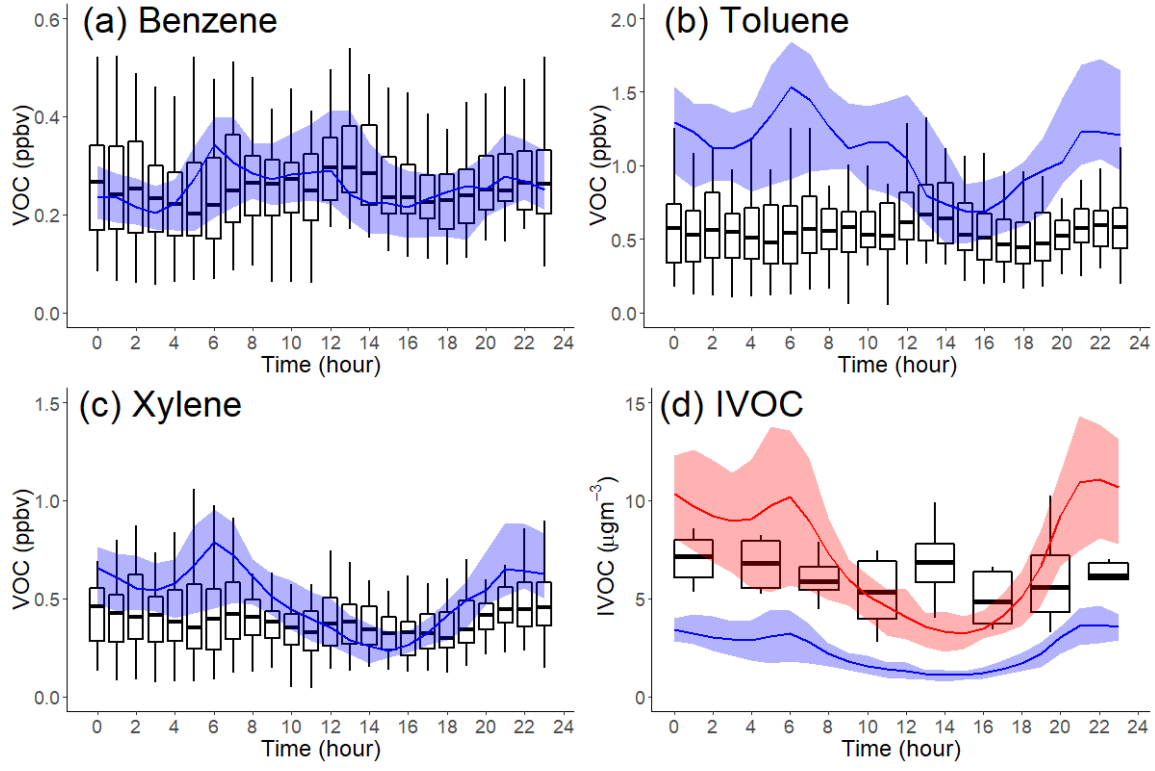

Figure 4: Comparison of measured (boxplot, solid box denotes 25th to 75th percentiles and whiskers denote 10th to 90th percentiles) and modelled (line, shaded area denotes 25th to 75th percentiles) diurnal patterns in Pasadena, CA during CalNex for species: (a) benzene, k_{OH} = 1.22 × 10 $^{-12}$ cm^3 molec^{-1} s^{-1} (b) toluene, k_{OH} = 5.63 × 10 $^{-12}$ cm^3 molec^{-1} s^{-1} (c) xylene, k_{OH} = 1.36 - 1.87 × 10 $^{-11}$ cm^3 molec^{-1} s^{-1} and (d) hydrocarbon IVOCs (blue: Case 2, red: Case 3), k_{OH} = 1.55 – 7.56 × 10 $^{-11}$ cm^3 molec^{-1} s^{-1}.

https://doi.org/10.5194/acp-2019-986
Preprint. Discussion started: 30 October 2019

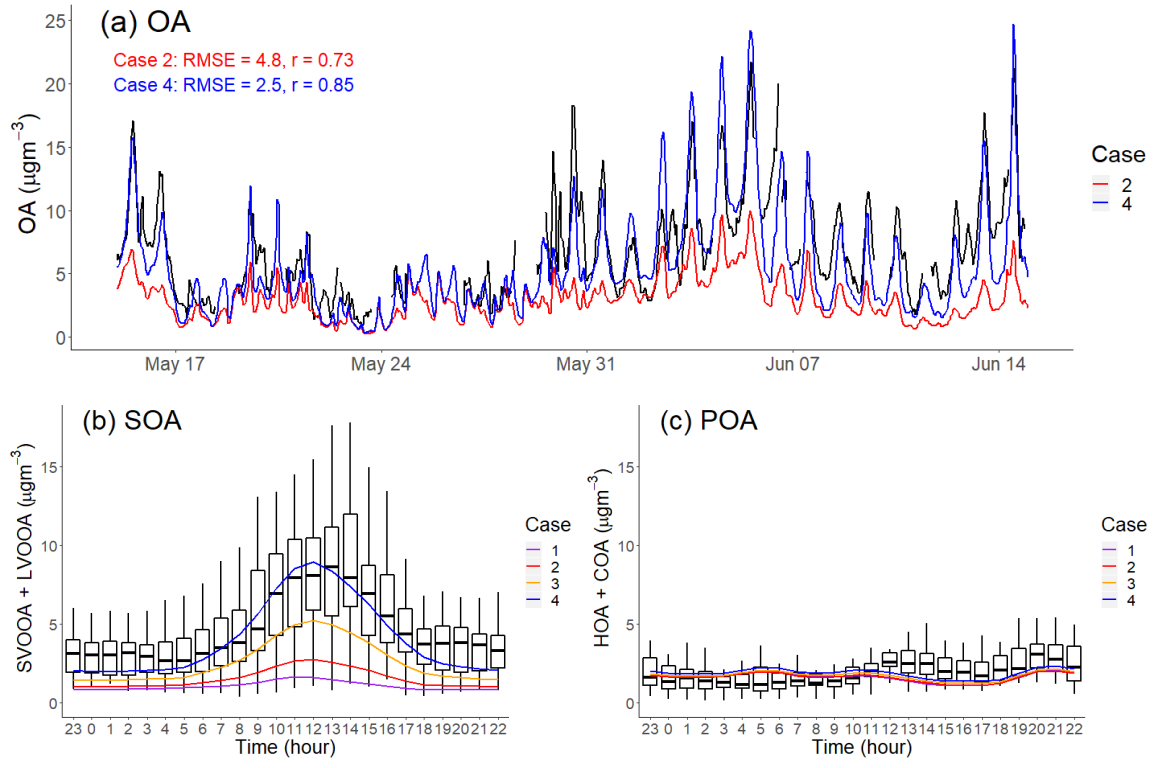

Figure 5: (a) PM_1-OA component hourly-averaged time series of measured data and model output in Pasadena, CA during CalNex campaign. (b, c) Diurnal pattern of measured and modelled POA and SOA mass concentration in Pasadena, CA during CalNex.

https://doi.org/10.5194/acp-2019-986
Preprint. Discussion started: 30 October 2019

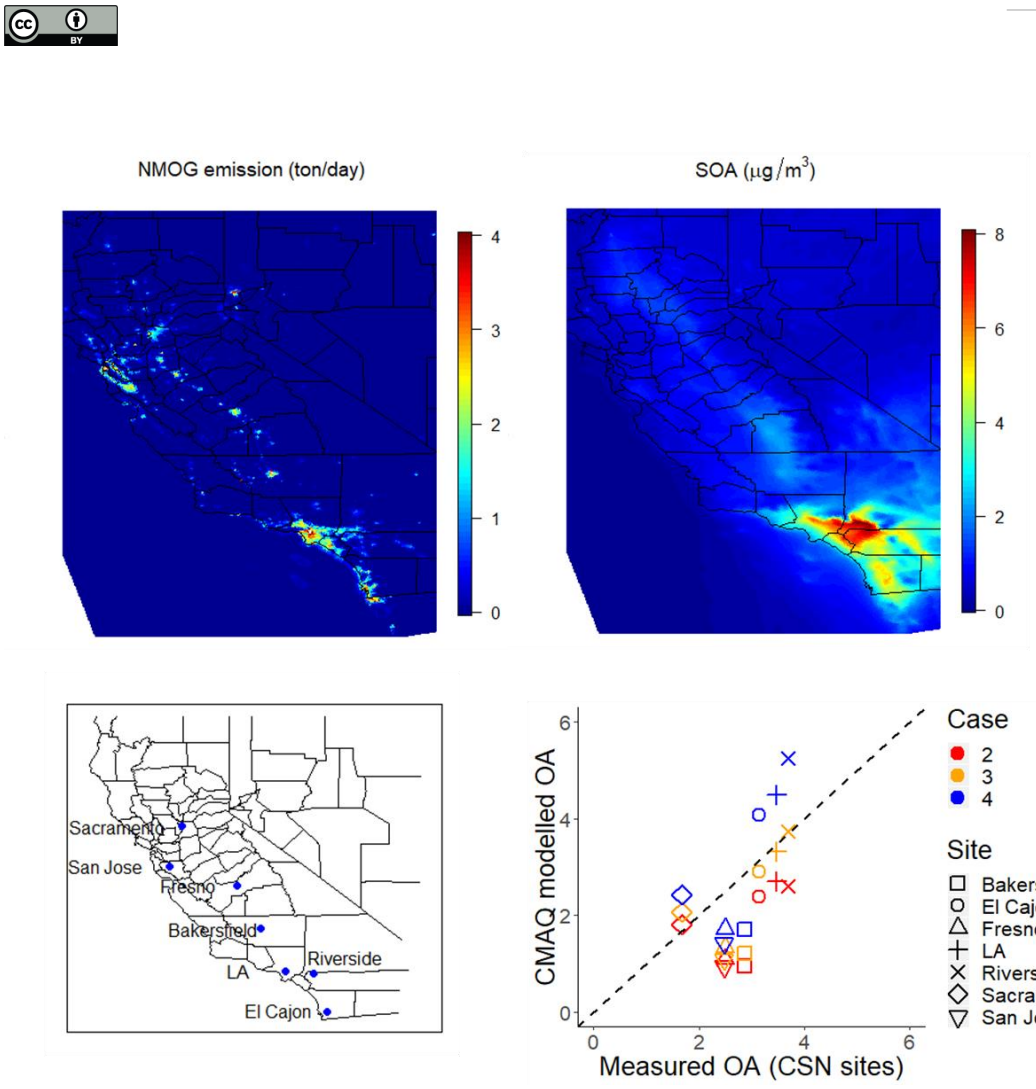

Figure 6: (a) Campaign-average NMOG emissions (ton per day) in emission inventory. (b) Modelled campaign-averaged SOA concentration in Case 4. (c) CSN sites in CA. (d) Comparison of modelled OA to measured OA (OC*1.8) at CSN sites in California.